J Solid State Electrochem (2008) 12:609–642
DOI 10.1007/s10008-007-0500-4

ORIGINAL PAPER

Pt–Ru electrocatalysts for fuel cells: a representative review

Oleg A. Petrii

Received: 5 February 2007 / Revised: 14 December 2007 / Accepted: 14 December 2007 / Published online: 23 January 2008

Abstract Three periods of Pt–Ru research are considered step-by-step: the initial period after discovery (1963–1970); observation and classification of basic tendencies (like the effects of composition, segregation, structural features on the activity; up to 1990); nanostructural studies and molecular level consideration of electrocatalytic phenomena in combination with advanced applied studies of materials, mechanistic, and applied aspects (after 1990). The main idea of this review is to balance various aspects of Pt–Ru electrochemistry related to material science and electrocatalysis as well as to remember the early basic results being of importance for future understanding of Pt–Ru functional properties.

Introduction

The second half of the twentieth century provided the outstanding progress in creation and improvement of various electrode materials as well as condensed ionic systems and membranes [1]. Among electrode materials, platinum–ruthenium catalysts for direct methanol fuel cells (DMFC) are widely recognized. These catalysts also found successful applications in reformate-air fuel cell. For this device, the fuel is conversed from methanol or hydrocarbons by means of reforming process and contains up to several percent of CO along with H_2 and CO_2. More than a thousand of papers concerning fabrication and studies of Pt–Ru catalysts can be already found in the literature.

Pt–Ru system had attracted serious attention already at the end of nineteenth century. Let us remind that ruthenium had been discovered in 1844 by K. Klaus in Kazan University, and the study of anodic ruthenium dissolution had been available already in 1868 [2]. Pt–Ru alloy (10 wt% Ru) had been mentioned for the first time as the thermocouple material [3]. The early physico-chemical studies of this system appeared in 1930s [4, 5]. During the post-war period, the pronounced synergetic effects were found for alloys containing 5–10 wt% of ruthenium in respect to liquid phase hydrogenation [6], isomerization [7], and catalytic CH_4–D_2 exchange [8] (some synergetic effects were also reported for the latter process on Pd–Ru [9]). As publication of [8] contemporized the period of the arising interest to fuel cells with organic fuels, it stimulated the electrochemical studies of Pt–Ru catalysts. This concerns at least the motivation of our study [10], which gave rise to subsequent series of Pt–Ru studies of 1960s [11–20].

In a huge number of Pt–Ru publications, the review [21] is frequently cited as a source of comparative data on electrocatalytic activity of platinum black and noble metal alloys in respect to methanol oxidation (Table 2 in [21]). Usually, nobody pays attention to the fact that this table is reproduced from the report of Adlhart and Hever [22] completed by the authors during the period from October 1963 to March 1964. The data reproduced in [21] are given for methanol solutions in 1 M H_2SO_4 at 100 °C and current density 20 mA/cm^2. According to these data, the strongest synergetic effects were found for platinum alloys with ruthenium and molybdenum as well as for ternary Pt–Ru–Mo alloy. The studies of Adlhart et al. related to platinum

---

Dedicated to Professor Teresa Iwasita, as a token of her remarkable contribution to electrocatalysis.

O. A. Petrii (✉)
Department of Electrochemistry, Moscow State University,
Leninskie Gory 1-str.3,
Moscow 119992, Russia
e-mail: petrii@elch.chem.msu.ru

alloys with ruthenium, osmium, and relative elements resulted in a number of papers and patents [23–26]. These publications are practically never cited nowadays. The paper [10] is only scarcely mentioned, while more usual citation [12] operates with the data from [10]. Another rarely cited paper is [27], which summarizes the results on the activities on platinum metal alloys and gold alloys with platinum metals in respect to methanol oxidation at 25 and 85 °C and current density of 50 mA/cm^2. Meanwhile, during the early Pt–Ru period, the Batelle group provided one of the most extensive studies of platinum modification by the majority of the elements existing in the periodic table to find the most suitable catalyst for organic fuel oxidation [28].

This review contains consideration of three periods to be marked out for the studies of Pt–Ru catalysts. The early period covers 1963–1970; it can be named rosy or romantic period in the history of Pt–Ru catalysts. The most important results of that period are compared below with some data of the recent decade. One should note that despite extremely intensive later research in the field, some data of the early period found themselves beyond the frames of active interest and still remain unique. During the second period (1970–1990), numerous novel approaches were developed to the studies and fabrication of Pt–Ru catalysts. Finally, the modern period corresponds to the shift from well-characterized alloys to alloyed and modified nanoparticles characterized at atomic level. These trends are also accompanied by the closer interrelation between design of nanostructures and fabrication of real catalysts for methanol fuel cells, with accenting DMFC problems (especially for the most prospective methanol fuel cells with polymer electrolytes). It is evident that the indication of years given above is arbitrary, and three periods are not separated by any sharp time boundaries.

Another goal of this review was to consider some data for ruthenium electrode, with a special emphasis on the conditions of ruthenium stability and valent state under DMFC operation conditions. It should be stressed that Ru is also the basic element of the other electrode materials of great practical importance [1], namely oxide ruthenium–titanium anodes for chlorine electrolysis and ruthenium dioxide electrodes of supercapacitors.

A number of reviews published in the course of the development of Pt–Ru area (see [29–33] for example) summarize the data of various periods and sometimes cover also other systems. However, even the series of reviews presented in the handbook [33] can be hardly considered as the integrate despite their evident helpful content (as these reviews give also a chance to compare the views of various authors on the problems of fabrication and utilization of Pt–Ru catalysts). Moreover, because of extremely rapid development of the field, these recent reviews already fail to reflect the current situation. This review[1] also does not pretend to complete description; it is aimed exclusively to presentation of the most reliable and essential findings as well as to fixing the pioneering findings and studies.

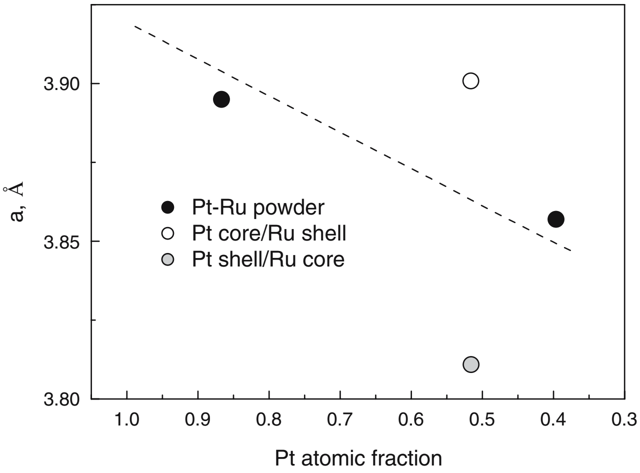

Fig. 1 Lattice parameter variation with Pt atomic fraction: Pt–Ru powder prepared using the borohydride technique [15] (*black solid symbols*), data of Vogel et al. [34] for Pt–Ru colloids (*dashed line*), and computational results for Pt(core)/Ru(shell) (*open symbols*) and Pt (shell)/Ru(core) (gray *solid symbols*)

The most important results of 1963–1970

The most detailed studies of the early period concern mixed Pt–Ru electrodeposited materials [10–20]. These electrodes were prepared by galvanostatic deposition from H_2PtCl_6 + $K_2Ru(NO)Cl_5$ solutions using platinum foil or gauze as the supports. In general, the deposit thickness was of approximately several microns. The deposit/bath composition ratio close to 1:1 was found using ^{106}Ru radiotracer technique [11]. Parallel studies involved the electrodes prepared from Pt–Ru powders resulting from chemical deposition with $NaBH_4$ reductant, Raney Pt–Ru catalysts, the catalysts on carbon and titanium carbide supports, and metallurgical Pt–Ru alloys.

Figure 1 presents the lattice parameter for powders obtained by means of chemical deposition as compared to parameters calculated for Pt–Ru in the absence of segregation phenomena [34] as well as for strongly segregated Pt (core)/Ru(shell) and Pt(shell)/Ru(core) nanosize catalysts. The dispersed materials studied in [10–20] demonstrated crystallographic features close to the absence of segregation and typical for bulk Pt–Ru materials.

Typical tendencies for various regions of cyclic voltammograms obtained for Pt–Ru electrodes with the increase of

---

[1] The basis of this review is the lecture "Ru-containing catalysts—a very long story" presented at 55th ISE Meeting in Tessaloniki, September 2004.

Ru content (Fig. 2) consist in (1) a gradual decrease (and later disappearance) of the maximum related to strongly bonded hydrogen; (2) current increase in the “double layer” region induced by earlier oxygen adsorption, and (3) more and more irreversible oxygen adsorption. These tendencies reported in [17] were later confirmed for other types of electrodeposited Pt–Ru and for numerous catalysts of another origin. Recent comparative study of electrodeposits fabricated at various constant potentials [35] demonstrates that deposition potential affects not exclusively the true surface area of dispersed Pt–Ru but also its stability and ageing behavior under various conditions.

The early papers on Pt–Ru electrodeposits collected a lot of detailed data concerning the kinetics of methanol oxidation [17, 19], with special attention to uncover the mechanistic criteria and to optimize the catalyst composition for various operation conditions.

According to [36], the most important mechanistic criteria are (1) Tafel slope of the steady-state polarization curves and (2) pH dependence of the reaction rate at constant potential. These features were preferentially studied; in addition, the effects of reactant concentration were obtained, the initial and steady-state oxidation rates were compared, and the latter were also considered jointly with the oxidation rates of methanol chemosorption products. The electrochemical study of the nature of these products [16] led to conclusion about deep dehydrogenation of methanol molecules in the course of adsorption, with forming the species of stoichiometry close to HCO (however, the accuracy of this conclusion is rather low because of strong intersection of hydrogen and oxygen adsorption regions for the catalyst under study). To finalize the list of what was studied, we should also mention the analysis of products for methanol oxidation at various potentials and the polarization curves measured for formaldehyde and formic acid electrooxidation.

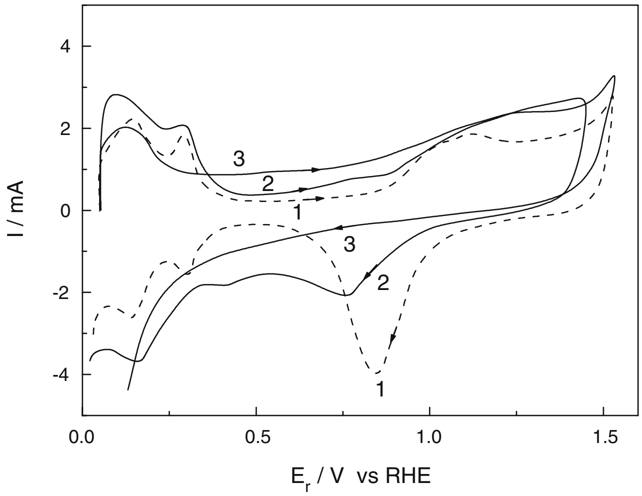

Fig. 2 Typical cyclic voltammograms of platinized Pt (*dashed*, curve *1*) and compact Pt–Ru alloy containing 10 and 30 wt% Ru (curves *2* and *3*, respectively) measured in 0.5 M H_2SO_4 solution, scan rate 5 mV s^{-1} [18]

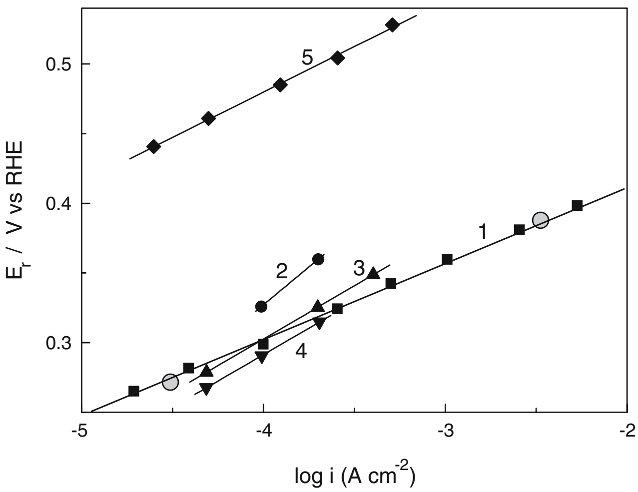

Fig. 3 Steady-state polarization curves of methanol oxidation on electrodeposited Pt–Ru (10 wt% Ru) (*1*), Raney Pt–Ru alloys (5, 10, and 20 wt% Ru, curves *2*, *3*, and *4*, respectively) and platinized platinum (*5*) [15]. 0.5 M H_2SO_4+0.5 M CH_3OH. *Points*: data for Pt–Ru prepared by sol–gel technology [37]

The catalysts studied in the 1960–1970s demonstrated high activity in respect to methanol electrooxidation. These electrodeposits are highly competitive with more characterized Pt–Ru materials reported later and considered nowadays as being the most active. Figure 3 presents the comparison of the steady-state polarization curves of methanol oxidation on Pt–Ru electrodeposit [20] and on the most active (under stationary mode) Pt–Ru catalyst fabricated by means of sol–gel technology [37]. Recent tendency of more detailed studies of catalysts under steady-state polarization should be specially marked; it results from closer interaction of basic electrocatalysis and applied fuel cell projects. Unfortunately, cyclic voltammetry dominated in the course of the second and third periods of Pt–Ru research, and the majority of reported data correspond to certainly non-steady-state registration modes.

According to [20], the regions of polarization curves at low potentials are probably pH-independent in the interval of pH 0.3–2.3 (Fig. 4) if the potentials are referred to the reversible hydrogen electrode (RHE) in the same solution. A slight increase of the oxidation rate is observed at higher pH. This effect can be attributed to the increased surface coverage with the active forms of adsorbed oxygen species in less acidic solutions. The observed pH effects and Tafel slope of about 60 mV find the simplest explanation under assumption of slow chemical interaction of methanol adsorption products with OH-like adsorbed species resulting from fast underpotential discharge of water molecules (this conclusion is related exclusively to steady-state oxidation and low anodic potentials; Scheme 1).

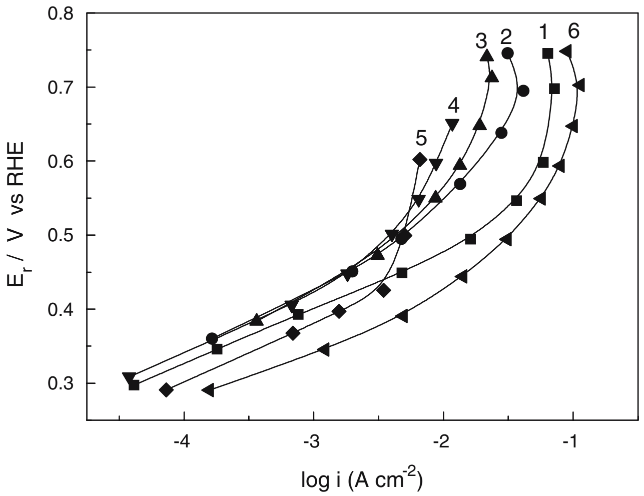

Fig. 4 The effect of pH on the steady state polarization curves of methanol oxidation on electrodeposited Pt–Ru (15 wt% Ru). 3 M CH_3OH in 0.5 M H_2SO_4 (pH 0.3) (curve *1*), sulphate buffer solutions (pH 1.0, 1.3 and 2.3 for curves *2*, *3*, and *4*, respectively), NaOH + Na_2SO_4 (pH 12.4 and 13.6 for curves *5*, *6*, respectively). All currents are related to geometric surface areas

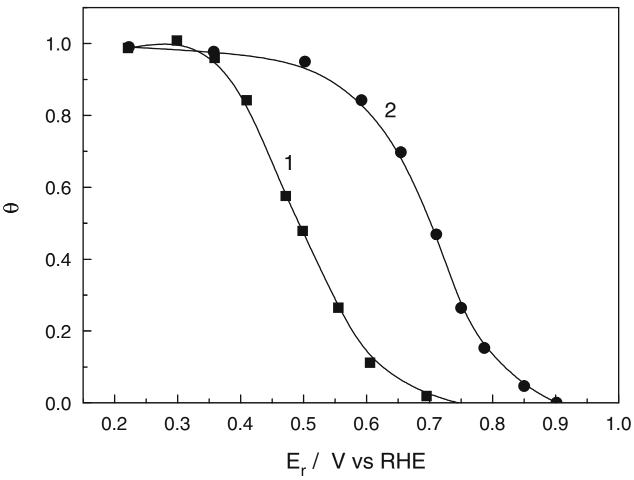

Fig. 5 The potential dependence of the steady-state surface coverage with methanol chemosorption products for electrodeposited Pt–Ru (15 wt% Ru) (*1*) and platinized platinum (*2*). Adsorption from 0.5 M H_2SO_4+0.05 M CH_3OH solution, with subsequent washing and surface coverage determination in supporting 0.5 M H_2SO_4 solution [17]

For constant surface coverage with $(CH_3OH)_{ads}$, this scheme provides the following kinetic equation:

$$i = \text{const}\ \exp(FE_r/RT), \tag{1}$$

where E_r is potential vs RHE in the same solution.

The validity of assumption of constant surface coverage with $(CH_3OH)_{ads}$ at low anodic potentials found indirect confirmation from the data on the amount of strongly chemosorbed organic species after washing the electrode to move away the dissolved methanol (Fig. 5). As one can see from Fig. 5, the region of $(CH_3OH)_{ads}$ electrooxidation on Pt–Ru is shifted for approximately 0.2 V towards less positive potentials as compared to oxidation on Pt, i.e., the overvoltage of this process decreases in the same manner as for oxidation of dissolved methanol. To confirm this statement, we compared the polarization curves of dissolved and adsorbed methanol oxidation (Fig. 6), providing a basis to assume a similar mechanism of both processes. The increase of oxidation rates of adsorbate when going from Pt to Pt–Ru was reported later by various authors.

Scheme 1 is currently accepted by the majority of people working with Pt–Ru catalysts for methanol oxidation. Detailed elaboration of this scheme now attracts modern quantum chemical approaches for modeling the adsorption of reacting species at heterogeneous electrode surface. Frequently used name of Scheme 1 in relation to methanol oxidation is Langmuir–Hinshelwood scheme.

It was well documented already in the studies of 1960–1970s that the adsorption of organic species on platinum group metals satisfies the model of the uniformly inhomogeneous catalyst surface (so-called Temkin conditions). The latter consideration agrees with the dependence of methanol oxidation rate on its bulk concentration c: The observed Tafel region corresponds to the following equation:

$$i \sim c^n \tag{2}$$

with $n<1$, corresponding to Temkin conditions.

For initial period of potentiostatic methanol oxidation, the slow step is most probably methanol adsorption accompanied by dehydrogenation [in contrast to slow step (1b in Scheme 1) under steady-state conditions]. Dehydrogenation is followed by the fast ionization of thus formed hydrogen adatom. The rate of this reaction was estimated from analysis of current transients registered after methanol injection to supporting solution under constant potential mode. Hydrogen ionization current arising at low potential in the course of injection are several orders higher than the steady-state currents and undergo a sharp decrease when the methanol adsorption products are accumulating at the surface. The initial currents (extrapolated to zero time) are proportional to methanol concentration. An interesting fact is the Tafel-like behavior of dehydration current at potentials of hydrogen adsorption (Fig. 6), with the slope close to the slope of the steady-state Tafel polarization curve. The

Scheme 1 Key steps of methanol electrooxidation

$$H_2O \leftrightarrow OH_{ads} + H^+ + e \tag{1a}$$

$$OH_{ads} + (CH_3OH)_{ads} \rightarrow \text{reaction products} \tag{1b}$$

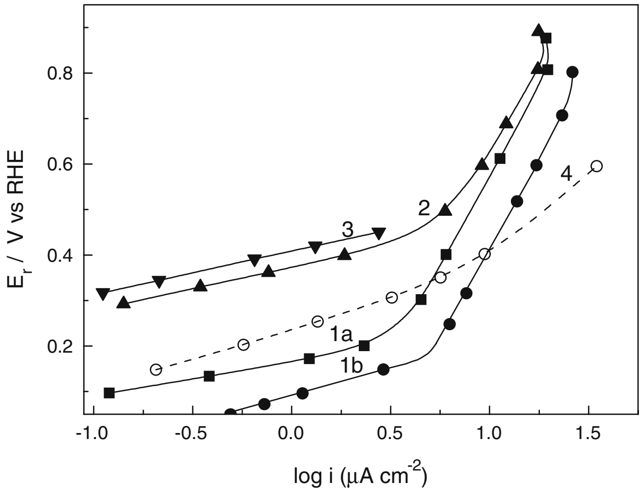

Fig. 6 Non-stationary (*t*=0) (*1a*, *1b*, *4*) and steady-state (*2*) polarization curves of methanol oxidation on electrodeposited Pt–Ru (15 wt% Ru) (*1a*, *1b*, *2*) and platinized platinum (*4*) [17]. 0.5 M H_2SO_4+0.1 M CH_3OH (*1a*, *2–4*), 1 M KOH+0.1 M CH_3OH (*1b*). Curve *3* corresponds to the oxidative desorption of the product of methanol adsorption on Pt–Ru (15 wt% Ru) in 0.5 M H_2SO_4 solution. All current densities are referred to the real surface area

potential-dependent rate of purely catalytic process can be explained by the dependence of hydrogen and oxygen surface coverage on the potential as well as by the changes in Ru atoms oxidation state. We shall demonstrate below that the specific features and mechanisms of dehydrogenation on mixed catalyst require further studies.

The difference in initial and steady-state methanol electrooxidation rates decreases with potential (Fig. 6), and both rates become very close at high potentials. For this potential region, we already observe much higher slope of polarization curve. Both facts provide true evidence of a different nature of the limiting step at high anodic potentials, probably coming to slow methanol adsorption. This assumption agrees well with the linear dependence of reaction rate on methanol concentration (in the range up to 1 M) observed for the same potential domain.

Several points should be stressed when comparing these data with the similar data for platinum electrodes.

Under identical conditions, the difference of initial and steady-state rates is more pronounced for Pt, demonstrating that poisoning by strongly bonded adsorbate is more pronounced in this case.

At low potentials, the rates of dehydrogenation on Pt and Pt–Ru are close (probably because of selective methanol adsorption on platinum centers), while dehydrogenation rate on Pt at higher potentials is higher. This observation can be attributed to the earlier oxygen adsorption in the presence of Ru and suppression of the adsorption rate by oxygen-containing species.

It also seems important that the electrooxidation rate of chemosorbed methanol on electrodeposited Pt–Ru at room temperature is only twice lower than the rate of electrooxidation of dissolved reactant, while the same difference for Pt approaches one order.

The steady-state rates of methanol, formaldehyde, and formic acid oxidation on Pt–Ru in acidic medium are rather close [17], while for Pt, their difference is pronounced. We suppose that similar composition of products formed in the course of these reactions on Pt–Ru results from this closeness of rates. As one can see from Table 1 (the data for low anodic potentials and reactant consumption of several percents), CO_2 (or CO_3^{2-}) dominate in all the systems.

The study of temperature effects (Fig. 7 [20]) leads to conclusion of the necessity of higher Ru content for the catalysts operating at elevated temperature, as it was confirmed in several recent studies considered below. The most interesting and surprising result is the high activity of pure electrodeposited ruthenium at *elevated* temperatures: At low potentials, it even exceeds the activity of Pt/Pt under the same conditions. The importance of this result became evident after a number of subsequent studies considered below. “Individual” ruthenium activity confirms that its addition to platinum can induce some electronic effects, not exclusively bifunctional. The reaction on pure ruthenium is hindered at higher anodic potentials, most probably because of earlier surface oxidation. Ruthenium was also found to be an effective catalyst of formaldehyde oxidation in alkaline solutions at high current densities. The special study of electrocatalysis by pure dispersed ruthenium should be considered as rather advisable.

Among the results obtained during the early period and still remaining little known, one should mention the methanol hydrogenation in the vicinity of zero RHE potential, with methane formation [15] (Table 2). The rate of this process increases with temperature.

In addition to organic reactants with a single carbon atom, ethanol electrooxidation on Pt–Ru was studied (Fig. 8). The observed synergetic effect is weaker than for methanol oxidation [15]. The synergetic effect for ethanol electrooxidation was confirmed later and contributed to the increased interest to direct ethanol fuel cell. The rates of

Table 1 Composition of the yields (%) of methanol electrooxidation products collected in electrolysis on Pt-Ru (15 wt% Ru) at room temperature

Solution	*E*(RHE) (V)	HCHO	HCOOH	CO_2
0.5 M H_2SO_4 + 0.5 M CH_3OH	520–530	2.5–3.0	9–11	86–88
	360–370	2.5	11	86.5
	450–465	1	68–71	31–28
1 M KOH + 0.5 M CH_3OH	325–335	1	15	82–85

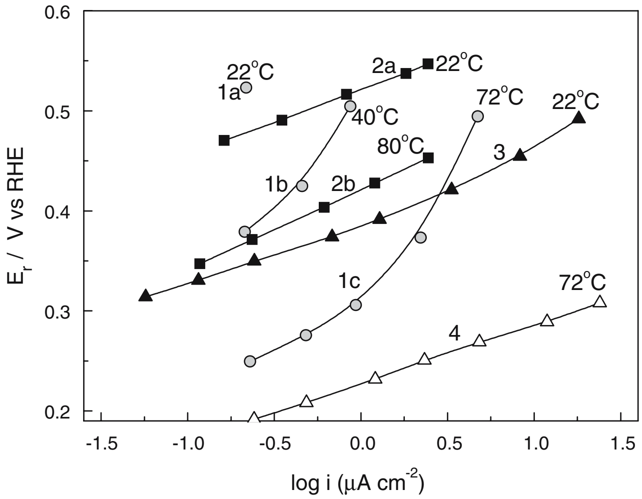

Fig. 7 Steady-state polarization curves of methanol oxidation on electrodeposited Ru (*1a–1c*), platinized platinum (*2a*, *2b*) and electrodeposited Pt–Ru (10 and 25 wt% Ru for curves *3* and *4*, respectively) [20]. 0.5M H_2SO_4+1 M CH_3OH at 22 °C (*1a*, *2a*, *3*), 40 °C (*1b*), 72 °C (*1c*, *4*), and 80 °C (*2b*)

ethanol hydrogenation appeared to be higher than for methanol [15]. Self-hydrogenation reactions were discovered for ethanol, propanol, and acetaldehyde in the course of slow establishment of the open circuit potential in solutions of these substances.

Methane electrooxidation on Pt was found to be inhibited by adding even very low amount of Ru [14]. This fact was explained by proceeding of the reaction at high anodic potentials, i.e., under conditions of strong inhibition of methane adsorption (the limiting step) by oxygen adatoms, as this effect tends to be aggravated in presence of Ru.

Adhlart and Hever [22] and Cohn and Adlhart [23] present the data on propane and butane electrooxidation on Pt–Ru, along with methanol reaction. The authors pay attention to the role of crystal size and porosity, the factors widely discussed later. They report that the fraction of large pores increases with Ru content, making the reactant penetration towards the internal electrode surface easier. The activity of such a catalyst in respect to propane and butane oxidation in 85 wt% H_3PO_4 appears to be higher than of pure Pt. Carbon-supported Pt–Ru (the most widespread type of currently applied and studied Pt–Ru materials) is described in [24]. Niedrach et al. [38] and McKee and Scarpellino [39] note for the first time the high efficiency of Pt–Ru electrode for electrooxidation of CO-contaminated hydrogen, forming a basis for later design of CO-tolerant catalysts for hydrogen–oxygen fuel cells. CO electrooxidation on Pt–Ru black is reported also in [40].

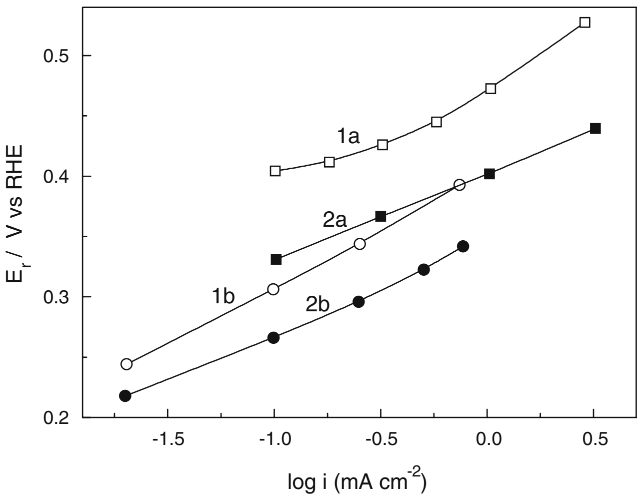

Fig. 8 Steady-state polarization curves of ethanol oxidation on platinized platinum (*1a*, *1b*) and electrodeposited Pt–Ru (10 wt% Ru) (*2a*, *2b*) [15]. 0.5 M H_2SO_4+0.5 M C_2H_5OH (*1a*, *2a*), 1 M KOH+ 0.5 M C_2H_5OH (*1b*, *2b*)

Table 2 Products of hydrogenation of organic compounds on Pt–Ru (15 wt%) at room temperature under open circuit [the yield (%) is given in brackets]

Fuel	E_i, (V) (RHE)	Products
Methanol	0.06	H_2(10), CH_4(90)
Ethanol	0.5	CH_4(92), C_2H_6(8)
	0.05	H_2(8), CH_4(55),C_2H_6(37)
Propanol	0.4	CH_4(35),C_2H_6(50),C_3H_8(15)
	0.06	CH_4(30),C_2H_6(40),C_3H_8(30)
Acetaldehyde	0.5	CH_4(95),C_2H_6(5)
	0.06	CH_4(89),C_2H_6(11)

E_i is initial potential.

The voltammetric study of Pt–Ru heat treatment effects [18] demonstrated Pt segregation at the surface. This phenomenon looks typical for metallurgical Pt–Ru alloys as well. The latter were also deformed using cold rolling, a procedure which has not changed their properties. Note that these alloys never demonstrated synergetic effects of the same order as dispersed materials. This conclusion (confirmed later by other authors) merits a more detailed study.

The nature of synergetic effect was poorly discussed in the literature of this period. Predominating hypothesis was a sharp difference in a number of unpaired electrons per one atom [8, 27]. Correspondingly, the electronic factor (named ligand effect in modern literature) was accented.

Electrochemistry of Pd–Ru system was minutely studied [13]. The specific feature of this system is its heterogeneity appearing at already 5 wt% Ru content [9] and affecting hydrogen sorption properties of palladium. Synergetic effect related to methanol electrooxidation was found to be even stronger than for Pt–Ru, but corresponding overvoltage remained higher than for Pt–Ru (probably due to low activity of Pd). One cannot exclude a possibility to find the effective ternary Pt–Pd–Ru catalysts with lower Pt content than in Pt–Ru of similar activity. The highest activity of Pd–Ru was observed in respect to formate in alkaline medium; it exceeded the activities of Pd and Pt–Ru. A patent for Pd–Ru catalyst for fuel cells became available in 1973 [41]. Hydrogenation of dimethylethynylcarbinole on alumina-supported Pd–Ru was studied in [42].

Oxygen electroreduction on Pt–Ru was also tested long ago [43, 44]. This problem is of special interest now because of discovery of ruthenium crossover, with subsequent Ru deposition at the oxygen electrode and deterioration of fuel cell with polymer membrane.

A separate group of Ru and Pt–Ru early electrochemical findings is formed by surface thermodynamic studies. Free charge dependence on the electrode potential [19] demonstrates a systematic shift of the potential of zero free charge (pzfc) towards more negative values when adding Ru to Pt. In 0.01 M HCl+1 M KCl solution, the value of pzfc was shifted for 60 mV at already 10 wt% Ru content. For pure Ru, pzfc founds itself in the region of molecular hydrogen evolution. Only so-called inverted pzfc can be found experimentally, which corresponds to the oxidized surface. Isoelectric potential shifts demonstrated the appearance of adsorbed oxygen on Ru at extremely low potentials. It is specially pronounced in alkaline solution: The amount of adsorbed oxygen exceeds the amount of adsorbed hydrogen at already 0.1 V RHE.

The early data on Pt–Ru electrochemistry listed above demonstrate that a number of results published during the first period are still of present-day importance. However, it should be stressed that these data obtained for electrodeposited Pt–Ru can be hardly extended automatically to other types of catalysts.

In addition to Ru alloys with Pt and Pd, other Ru-containing systems were studied during the same period. Ru–Ta electrode for fuel cell applications was proposed [45]. The attempts to oxidize the molecular hydrogen and to enhance hydrogenation of some organic substances using Ru–Ni alloy were reported [46]. The alloys of Ru with Rh [47, 48] and Ir [49] were also tested. Doping of some metals (Pb, Tl, Ag) with Ru was found to affect strongly their corrosion and electrochemical behavior [50].

We should also mark more general keen interest to the studies of Ru metal, Ru compounds, and Ru electrochemistry in the 1960s. A basic scheme of Ru oxidation was proposed [51]. The advances of Ru chemistry were reviewed in relation to analytical applications [52]. The redox potential for Ru(II)/Ru(III) couple was determined [53], and the reduction of various Ru complexes to Ru metal was studied [54, 55]. The voltammetric response of smooth ruthenium [56] and thin ruthenium films [57], hydrogen evolution on smooth ruthenium [58], catalytic hydrogen evolution on Ru clusters [59], ruthenium electrocrystallization [60] and its corrosion behavior [61–64] were discussed. The research group in Moscow University worked out a number of techniques to prepare the ruthenium electrodes with high surface area, provided the estimate of their true surface area, and studied the effect of heat treatment on the properties of dispersed ruthenium, including electrochemical hydrogenation of various organic compounds and poisoning of these reactions with arsenic and mercury [65–72]. Temperature effect on the adsorption properties of ruthenium black was also studied in [73].

1970–1990: new approaches appear

It became clear that the second Pt–Ru period started when Motoo's group confirmed a very high electrocatalytic activity of Pt–Ru and demonstrated a possibility to provide the same activity by surface modification of platinum with Ru adatoms [74–78]. Motoo and coworkers introduced the term "electrocatalysis by adatoms" for electrocatalytic phenomena resulting from surface modification with foreign adatoms.

Various techniques to modify platinum surface with adatoms were initially summarized in [79]. This approach was later widely applied (see [80] for review and some comments below). The current state of the problem is presented in [81].

When considering a possible nature of high Pt–Ru activity, Watanabe and Motoo [77, 78] formulated the mechanism of bifunctional catalysis. According to their idea, the ruthenium centers are responsible for generation of active oxygen species, while platinum centers keep the adsorbed methanol species. Thus, the spatial separation of the chemosorbed methanol and oxygen was assumed. For confirming the bifunctional mechanism, the authors reported a good correlation of the number of Pt–Ru pairs (calculated in frames of Bragg–Williams and Fowler–Guggenheim order–disorder theory) and catalytic activity for CO electrooxidation. In particular, the highest activity corresponded to the maximum number of Pt–Ru pairs. This analysis favored further predominating considerations of geometrical factors in Pt–Ru electrocatalysis, with minor attention to the obvious independent factor, i.e., the electronic state of platinum atoms at the surface (strongly modified in the presence of ruthenium).

Like any simple and transparent idea, the bifunctional mechanism was immediately accepted and recognized. It still predominates in Pt–Ru research, remaining the basic model of synergetic effect (see the third section of this review).

In their extensive series of papers on electrocatalysis by adatoms, Motoo et al. considered two groups of adatoms, namely (1) oxygen-adsorbing (or oxophylic) and (2) oxygen-non-adsorbing (the latter were assumed to adsorb oxygen at the same potentials as the supporting metal, or even at higher potentials). For Pt support, group (1) involved Sn adatoms catalyzing methanol electrooxidation along with Ru. Taking into account the mechanism of methanol oxidation, the authors of the series formulated their assumptions concerning the difference in the effect of (1) and (2) types of adatoms and emphasized the distinctions of bifunctional mechanism and earlier proposed redox mechanism of electrocatalysis by Mo [82].

In parallel with mechanistic advances, a lot of important findings of the second Pt–Ru period are related to optimization of materials. Application of Petrow–Allen technique by Watanabe et al. [83] resulted in the fabrication of highly dispersed supported catalysts consisting of clusters and demonstrating true surface area up to 80 m^2 g^{-1}. This technique of supported catalysts preparation was later widely used (with certain modification). Simultaneously, the optimization of Pt–Ru deposition on carbon supports became a subject of a number of studies [84–86].

The phase diagram of Pt–Ru system was completed [87]; in agreement with the earlier data [4, 5], it appeared to be rather simple, with an fcc phase at Pt concentration above 40 at.%, an hcp phase at Pt concentration below 20 at.%, and a two-phase region in between. An attempt was done [88] to consider the specific features of hydrogen and oxygen adsorption on compact Pt–Ru alloys, with taking into account possible two-phase composition in a certain interval of Ru content.

The second period attracted more attention to various reactions on Pt–Ru electrodes besides methanol oxidation. In particular, Beden et al. [89] started the research in this area, in particular by demonstration of high activity of Pt modified by Ru adatoms in respect to ethylene glycol oxidation. This group remains very active in the same field nowadays. A number of DMFC development problems were considered by McNicol [90].

The high activity of Pt–Ru system in reactions of various organic fuels was confirmed in [91, 92]. Some data appeared on ammonia oxidation [93] and nitromethane reduction [94] on Pt–Ru.

The problem of Pt–Ru activation was touched by McNicol and Short [95]. In agreement with the previous data on the effect of heat treatment under inert atmosphere on the electrochemical behavior of Pt–Ru alloys [20], voltammetric manifestations of segregation were also observed. Heat treatment in hydrogen resulted in Pt segregation because of stronger hydrogen adsorption on Pt. In contrast, heat treatment in oxygen resulted in segregation of Ru because of stronger oxygen adsorption on this metal. In general, these data lead to conclusion widely accepted in heterogeneous catalysis. According to this experience, any manipulations with binary catalysts, like heat treatment under various conditions, transfer (to reactors or spectrometer chambers) in air, contact with electrolyte solution or its replacement, as well as realization of electrocatalytic process itself, can affect the surface composition and by these means to change the activity.

The studies of fabrication conditions on the surface composition of silica- and alumina-supported Pt–Ru clusters highlighted the role of specific ligand exchange interactions of the precursors with the surface molecular groups of the supports. These interactions can result in the formation of well-defined cherry-like structures and core strongly enriched in Ru or Pt [96]. The possibility of similar structure-affecting mechanisms cannot be a priori ignored for, to say, Pt–Ru deposition on carbon supports, with their rather specific surface functional groups.

A general problem recognized in the course of the second period is the nature of Pt–Ru tolerance in respect to CO. It was confirmed [97] that the presence of Ru decreases the overpotential of CO oxidation onset (the equilibrium potential for CO/CO_2 couple is about 0.1 V RHE). At the same time, slower poisoning was discussed as the reason of increased catalyst activity when operating in CO-contaminated hydrogen [98].

Among the novel trends in design of Pt–Ru catalysts observed during this period, the development of techniques to deposit catalyst particles into solid polymer electrolytes (SPE) should be mentioned, especially Nafion modification [99, 100]. For catalysts preparation on polymer membranes, the role of charge of complex precursor specie was discovered, as it affected reagent penetration inside polymer matrix [101].

The second Pt–Ru period coincided with a peak of electrochemical and corrosion studies of amorphous materials stabilized by non-metallic additives. The attempts to fabricate amorphous Ru-containing catalysts and to test their activity in methanol electrooxidation were made [102, 103]. However, this approach found poor further development, probably because of too complex preparation techniques and less significant advantages of amorphous catalysts as compared to other types of materials.

Some other synthetic routs were also applied to Pt–Ru catalysts, including exotic: Ru implantation in Pt [104], Pt implantation in RuO_2 [105], sputtering of Ru clusters of various sizes [106], spraying of oxide powders, mixed and suspended in toluene, on Au support [107].

Studies of Pt–Ru alloys electrodeposition were also continued during the second period using chloride bath and galvanostatic mode [108]. The prepared electrodes demonstrated the same type of voltammetric features as reported in earlier studies [17]. The important point is a possibility to deposit metallic ruthenium only in the presence of platinum compounds in the bath. The overvoltage decrease for ruthenium discharge results from the energy of alloy formation. Cathodic currents observed in purely ruthenium bath should be most probably assigned to Ru(III)/Ru(II) reaction.

Chlorine evolution on platinum and its alloys, including the alloy with 17 at.% Ru, was studied in [109]. The authors were looking for correlation of chlorine evolution rate (or exchange current density) and the degree of d-character or the work function and found linear correlation. Alloy with Ru demonstrated lower activity as compared to Ir and Pd alloys with Pt. Hydrogen adsorption and evolution [110] were studied on compact Pt–Ru, as well as nitroethane adsorption and electroreduction [111]. In particular, no adsorption of nitroethane on pure Ru was found.

Characterization of Pt–Ru catalysts with the use of physical techniques started in the second period and later found widespread occurrence. Optical techniques were initially involved, as they were undergoing fast development in the 1970s. Ellipsometry of Pt–Ru and Ru electrodes [112] confirmed the early formation of oxygen-containing adsorbates at Ru centers—at already 0.25 V RHE. Ruthenium oxides were discovered starting from 0.95 V, while manifestations of ruthenium dissolution in acidic medium appeared only at potentials exceeding 1.3 V RHE. We should also mention one of the early X-ray photoelectron spectroscopy (XPS) applications to Ru [113] and UV–vis study [114].

Electrochemistry of pure ruthenium was studied actively during the second period. The first attempts to study Ru single crystals electrochemistry were reported [115, 116]. The Pourbaix diagram of Ru was specified [117] with attraction of data from [118, 119] and analysis reported in [120].

The important results on ruthenium electrodes were published by Conway and coworkers [121–124], still considered in relation to ruthenium oxidation at lower potentials (as compared to platinum) and types of resulting oxides. The interest to ruthenium oxidation induced publications of some other papers [125–128]. Ruthenium corrosion [129, 130] attracted a serious attention and was studied with the use of advanced techniques.

Hydrogen and oxygen adsorption on ruthenized platinum in acidic solutions was discussed in [131]. Hydrogen adsorption on ruthenium black at various solution pH was studied in [132]. The effect of Ru black dispersion on its adsorption and electrocatalytic properties was studied for the first time [133].

In the context of the study devoted to oxidation of molecular hydrogen on polycrystalline Ru [134], the assumptions concerning the possibility of hydrogen dissolution in ruthenium metal [123, 124, 135] were subjected to criticism.

Fast progress of electrochemistry of conducting polymers was accompanied by the attempts to deposit platinum group metals into polymer matrixes. The technique proposed in [136] results in Ru deposition into poly(4-vynil pyridine) film on glassy carbon, with providing high stability of metallic nanoparticles in acidic media and their activity in respect to hydrogen evolution.

Cu UPD was used for the first time in [137, 138] to characterize ruthenium deposited on platinum. The choice of Cu adatoms as the probes was motivated by the close atomic radii of copper (0.128 nm) and ruthenium (0.134 nm). This means that in the case of complete monolayer formation and under condition of exact surface stoichiometry, a chance appears to determine true surface area from the charge of Cu desorption. Such a possibility was confirmed for ruthenium materials with roughness factors below approximately 30, while for rougher surfaces, the multilayer growth of copper started before completion of the first monolayer.

Additional complication resulted from early oxygen adsorption and competition of copper and oxygen for positions at the surface. According to [137], electrochemical Cu UPD on Ru is similar to thermal deposition of Cu on a single crystal (0001) plane of Ru studies by low-energy electron diffraction (LEED), Auger spectroscopy, thermodesorption, and work function measurements by Christmann et al. [139].

The comparative study of Cu and Ag UPD on polycrystalline ruthenium was reported in [140], Tl and Pb adatoms behavior is described in [141], and data on Bi adatoms on ruthenium can be found in [142]. The transition from UPD to Ru–Ag alloy formation was studied in [143].

Along with characterization of surface oxidation states and hydrogen adsorption, the interest to study of more tiny interfacial phenomena was observed. Trasatti [144] discussed possible forms of adsorbed water on Ru, Rh, and Pt. The adsorption of chloride and sulfate anions on Ru was studied by Horanyi and Rizmayer [145] and Horanyi and Veres [146].

Oxygen evolution on ruthenium and ruthenium dioxide attracted serious attention [147–152], as well as ruthenium dioxide electrosynthesis. It is interesting to mention that the latter material was found to be suitable as a catalyst for hydrogen evolution [153, 154]. When testing it as the cathode material for hydrogen evolution, the authors found that copper adatoms do not form on dioxide centers, but exclusively on metallic ruthenium. At the same time, they observed bulk copper deposition on the dioxide, with the growth of separate clusters not affecting the rate of hydrogen evolution. According to [155], metal UPD is not typical for semiconducting oxide supports.

The increase of interest to applications of SPE in electrochemical devices prompted the studies of ruthenium oxide corrosion in the presence of SPE [156]. The dissolution under anodic polarization was found to depend on the exchange reactions with SPE, the presence of impurities in polymer membrane, the changes in local pH, and other phenomena.

The structure of the electric double layer on ruthenium dioxide was studied, including determination of the potentials of zero charge (in particular for single crystalline RuO_2 samples) [157–160]. Chemical modification of ruthenium oxides is reported in [161].

Basically, the Pt–Ru studies of the second period were less intensive, with major efforts spent for the studies of pure ruthenium and its oxides stimulated by applications of ruthenium–titanium dioxide anodes in industrial chlorine electrolysis[2]. Another reason was probably the prospect of rechargeable oxides application in supercapacitors. However, there are no doubts that the second period assured the starting points for large-scale Pt–Ru electrochemistry being one of the hot spots today[3].

Contemporary studies of platinum–ruthenium catalysts

Starting from the 1990s, the interest in Pt–Ru system has been rekindled, and a lot of research groups all over the world started with this system simultaneously. Several dozens of teams can be mentioned working now systematically in the field. They often have close collaboration and even form international groups despite typical research competition playing a stimulating role. The reason of this fast activation is the perception of the direct methanol fuel cell prospects (in view of both its miniaturized version for radio-electronic devices [164, 165] and vehicle applications). Current densities attainable with the use of Pt–Ru are estimated as sufficient for working out the fuel cells with power density above 2 kW m^{-2} [31].

National research programs opened now in USA, Japan, and a number of European countries are concentrated on DMFC with proton-exchange membrane (PEM) as solid electrolyte. Companies like Daimler–Chrysler, General Motors, Toyota, and Nissan are actively involved into research on electric vehicle application of DMFC.

As a result, a large-scale research and development of electrodes for practical applications, including optimization of the electrodes as well as membrane-electrode assemblies (MEA) and of fuel cells as a whole was started. Tests of MEA discover new problems induced by the compatibility of components and general design effects under certain operation conditions corresponding to necessary technological steps. Serious attention was also attracted to fuel crossover problem. The investigation in these new applied fields goes in parallel with the development of nanoelectrochemistry and electrochemical material science (with accenting nanostructured materials). Both of two new basic fields contribute to the progress in applications and simultaneously get rich due to technological advancements.

A sharp growth of basic Pt–Ru studies took place during the recent decades because the powerful physical techniques became more combinable with electrochemistry, and their application to surface and bulk electrode characterization resulted in the appearance of well-defined materials. The progress of single-crystal and nanoparticle electrochemistry was also of serious importance, providing new and new types of model systems and the next level of understanding the electrocatalytic phenomena. The studies of ruthenium single crystals demonstrated that this metal differs markedly from the other platinum metals and possesses some unique adsorption and electrocatalytic properties.

The studies of ruthenium oxides (first of all ruthenium dioxide) and non-stoichiometric oxohydroxides formed a separate field, with a number of specific techniques and modification approaches. This field should be considered in a separate review; we mention only one of the recent papers on ruthenium oxide optimization for supercapacitors [166] containing earlier references.

We avoid also the discussion of numerous ternary and more complex systems increasingly studied nowadays. Several binary systems relative to Pt–Ru are discussed below if their comparative consideration helps to understand the nature of electrocatalysis. Patents on Pt–Ru catalysts are also out of frames of this review.

Fabrication techniques and optimization of Pt–Ru

Novel techniques to fabricate highly dispersed catalysts appeared during the modern period, with a parallel improvement of previously known techniques. Two general tendencies can be marked out, namely the creation of catalysts for practical devices (“real” electrocatalysts of high surface area) and design of model Pt–Ru systems to discover the mechanisms of electrocatalysis and the reasons of CO tolerance.

The commercial Pt–Ru catalysts like E-TEK and Johnson Matthey became widely available, and their comparison with various homemade catalysts became a separate research direction. Thorough analysis of these commercial catalysts demonstrated that Vulcan XC-72-supported E-TEK catalysts are completely alloyed and contain no additional ruthenium phases (like RuO_x); this was concluded from high-resolution electron microscopy and X-ray microchemical analysis [167]. In addition to electrochemical experiments in half-cell configuration,

---

[2] Publication of monograph [162] devoted to ruthenium chemistry should be mentioned.

[3] State-of-the art in electrocatalysis at the beginning of the third period was vividly presented by Pletcher [163].

measurements with the use of MEA and MEA-based arrays (laboratory fuel cells) became generally used.

Classification of currently available Pt–Ru catalysts can be as follows: non-supported catalysts (including conventional alloys), templated catalysts and catalysts immobilized in various matrices, supported catalysts (including sputtered films and immobilized separated nanoparticles), and modified (decorated) flat surfaces including single crystalline. Two latter types, being of special interest for modeling the basic electrocatalytic phenomena, are considered below in a separate section.

Consideration of certain catalyst as supported or non-supported is sometimes ambiguous because any electrode material in a circuit requires some current collector. In what follows (and typically in the literature) a catalyst is named “supported” if its particles interact with support (current collector) just in the course of formation, and their catalytic behavior can depend on the nature and/or structure of support. However, in many papers, “supported” is used simply for catalysts being deposited on conducting surface in the course of fabrication.

When working out the strategies of electrocatalysts preparation, the following points are of most importance: the choice of precursors; the choice of deposition technique; the choice of support or electrode fabrication technique; and catalyst pretreatment activation. Anytime, the choice is directed to obtaining the highest activity for as low loading as possible, with simultaneous ensuring the best stability under any given operation mode. Simple and environment-friendly technologies are always desirable.

Precursors

The range of precursors became much wider during two recent decades. One of the tendencies was to exclude, to simplify, and/or to improve the procedures to delete the impurities resulting from precursor molecules. New platinum and ruthenium complexes with inorganic and organic ligands were proposed as the precursors [168–171]. Namely, [168], bimetallic Pt–Ru particles were prepared by co-deposition from two precursors, Pt(dba)$_2$ and Ru (COD)(COT)[4] dissolved in tetrahydrofuran (various ratios). Reduction with hydrogen was carried out at room temperature, and polyvinyl pyrrolidone was used to stabilize the particles of 1- to 1.5-nm mean size whose bimetallic nature was confirmed by infrared (IR) spectroscopy. For PtRu$_3$ composition, the interpenetration of the fcc and hcp network (twinning) was found.

Binuclear Pt–Ru complexes were synthesized [172, 173] and found to be opportune for the preparation of catalysts of fixed stoichiometry. Their additional advantage is the ability to provide a homogeneous distribution of platinum and ruthenium atoms along the support surface when the technique is applied to impregnation.

Supports

Optimization of supports attracted serious attention. Direct comparison of carbon-supported and unsupported Pt–Ru anodes in DMFC configuration demonstrate doubtless advantages of supported material (see, for example, [174]) first of all because of essentially lower metal expenditure. There are many independent reasons to use carbon supports for applications, so just the optimization of carbon supports became the most important branch of these studies. Various types of commercially available carbons were tested. The reasonable values of carbon-specific surface area and the role of porosity were addressed in detail in preceding studies of platinum catalysts, and the principle conclusions were applied to the choice of support for Pt–Ru preparation. Simultaneously, some novel types of carbons were tested, namely Sibunit family of less dispersed carbons. For Sibunit carbons, the effects of porosity and metal loading were well documented [175, 176]. Separated nanoparticles were found to coalesce with loading increase, forming first 2D and later 3D nanostructures of high defectiveness resulting from the presence of intergrain boundaries between nanoparticles. Defective regions appear to be long-lived and are assumed to be responsible for high catalyst activity.

Special emphasis was placed on precursor–support interaction determined by the nature of functional groups at carbon surface, as this factor strongly affects the subsequent behavior of catalyst. Much stronger interaction of carbon with ruthenium precursor (as compared to its interaction with Pt) was concluded in [177], and for carbon impregnated with precursor solution, this fact can, in its turn, affect catalyst chemical composition in the course of reduction. Lattice parameters of Pt–Ru alloys can be also affected by the presence of carbon (due to its penetration into the lattice). A general empiric approach is to use various types of carbons and to check their effect on the properties of the resulting catalyst.

Carbon nanotubes were tested as a novel support [178–183]. The technique was proposed to grow up the tubes at the surface of carbon cloth, with the subsequent deposition of Pt–Ru alloy in the presence of ethylene glycol (4.9–5.2 nm particles were formed) [180]. Composite material based on polypyrrol and multiwall nanotubes was proposed [184]. Lower Pt–Ru loadings are found when mesocarbon microbeds are used as support [185].

For some carbon materials, low stability of the supported Pt–Ru catalysts is found in methanol- and ethanol-contain-

---

[4] Abbreviations: dba—dibenzylidene acetone; COD—1,5-cyclooctadiene; COT—1,3,5-cyclooctatriene.

ing media. Even under ambient temperature conditions, metal is removed and forms catalyst suspension. The stability decreases with temperature and under ultrasound treatment of catalyst suspensions [186–191]. This leads to catalyst degradation, complications with controlling its composition and Ru content. Ruthenium tends to form ionic species in electrolyte, which later move to polymeric membrane and form the bonds with its sulfogroups, increasing by these means the membrane resistance [192, 193]. This phenomenon is assumed to be the reason of ruthenium crossover discussed below. The conditions providing carbon-supported catalysts stable in contact with solutions of alcohols were specially addressed in [190]. To stabilize Pt–Ru catalyst on carbon, the use of nonionic surfactants was proposed [194]. Possible improvement of Pt–Ru deposition on carbon supports are considered in [195–197].

Besides carbons, titanium gauze supports can be applied [198–201]. Titanium-specific feature is a possibility of electroless deposition. This material undergoes oxidation under fuel cell operation conditions and sometimes cannot be considered as the support in conventional sense (for example when Pt–Ru powder is mechanically attached to the support consisting of ordered TiO_2 nanotubes [202]). Hepel et al. [203, 204] proposed a novel method to prepare titanium dioxide with 20- to 80-nm pore diameter and used this material to support the electrodeposited Pt–Ru alloy. Both materials described in [202–204] are characterized by high loadings, and the role of the support requires further clarification. Thermal treatment was assumed to result in $PtRuTiO_x$ with less pronounced tendency to agglomeration [205]. Ni spheres were also applied [206]; good results were obtained for PtRu electrodeposited on metal foams [207].

When the rare earth oxides are added to reagents mixture, more dispersed catalyst is formed [208]. It is not completely clear whether these oxides can be considered as the supports. Deposition of PtRu into tungsten carbide template was proposed [209].

The development of miniaturized DMFC (so-called μ-DMFC) led to a new goal of studying Pt–Ru deposition on silicone supports. Thereupon, the prospects of using micro-electromechanical systems technology for design of systems for applications are opened [165, 210]. In [211], PtRu was deposited on SiO_2 nanowires grown on the surface of carbon paper.

Preparation procedures

The majority of Pt–Ru alloying techniques for preparation of dispersed electrocatalysts are based on thermal decomposition of the precursors, their chemical reduction, and electrodeposition. Ball-mill mechanochemical method [212, 213] was also applied by some groups. Recently, sonochemistry was applied successfully [214].

Various reducing agents were used for chemical deposition of Pt–Ru catalysts, namely hydrogen, sulfite, complex organic borohydrides, zinc, formaldehyde, formic acid [215], formate, inorganic borohydrides, hydrazine, tertathionate, $S_2O_3^{2-}$, alcohols and polyols (including ethylene glycol [216, 217], and polyethylene glycols [218]). Reduction with polyethylene glycol results in smaller particle size as compared to commercial E-TEK, but in lower activity (insufficient degree of alloying was assumed, or nanoparticles poisoning with organic species) [218]. Polyol techniques were actively optimized during the recent years [218–221].

Besides water, some non-aqueous solvents can be used for reduction. For tetrahydrofurane solution, stabilizing of nanoparticles with solvent was assumed [222]. Borohydride techniques appeared to be convenient and efficient, and new modifications of the procedure were proposed [223]. According to [224], the reduction of H_2PtCl_6 and $RuCl_3$ mixture with NaH_2PO_2 provides a catalyst of $Pt_{1.01}Ru_{0.98}P_{0.79}$ bulk composition with specific surface area exceeding the area of a standard E-TEK catalyst. The authors consider accumulation of phosphorus in the alloy bulk as the reason of particle size decrease (down to approximately 2 nm) as well as the reason of improved activity towards methanol and CO oxidation. However, more usual effect of accumulation of foreign component is catalyst deterioration.

Serious attention should be paid to reduction procedure itself, as its details affect a possibility to obtain a catalyst of desired Pt/Ru atomic ratio (at least in the bulk) containing no pure metals [225–227]. It is also important whether the complete deposition of metal is achieved; the answer depends on the reductant nature [228]. Alloying is usually tested by means of X-ray diffraction (XRD) and considered in terms of Vegard’s rule feasibility. An approximate alloy composition can be estimated from the lattice constant using this rule.

The reduction procedure is crucial for resulting particle size. For supported catalysts, it also affects particle distribution, in particular the distance between neighboring particles. More difficult and less controllable is the distribution of Pt and Ru positions at atomic level, whose role is stressed in the most recent papers [229].

A number of procedures to prepare Pt–Ru are so advanced that they can be considered as perfectly working technologies suitable for a large scale application.

First of all, it is true for sulfite techniques (Petrow–Allen, or Prototech, or sulphito-method) reported initially in [83]. A number of modifications were proposed to increase the stability of catalysts. In particular, Liu et al. [230] used sulfite complexes to prepare unsupported and carbon-supported Pt–Ru samples with high surface area. Arico et al. [231] used the mixtures of Pt and Ru sulfite complexes and found that higher Ru content induces the formation of smaller particles with correspondingly high specific area (up to 184 $m^2\ g^{-1}$ for $Pt_{40}Ru_{60}$). The highest activity towards methanol oxidation in DMFC with polymer membrane at 130 °C was found for Pt/Ru=1:1.

Dickinson et al. [232] developed the technique based on platinum and ruthenium carbonyl precursors, with deposition from *o*-xylene (solvent with a high boiling temperature) on Vulcan XC-72R. They were successful in obtaining homogeneous distribution of particles (mean size 2.5 nm) with rather narrow size distribution and activity close to activity of catalysts resulting from a standard sulphito procedure. Their technique also has technological prospects.

Good results are reported for catalysts prepared via modified Adams route, consisting in melting the mixture of target metal nitrates in excess of sodium nitrate, with subsequent washing of mixed oxides with water and their reduction under hydrogen atmosphere [233]. Mean size of particles appears to be 3–5 nm, but some portion of ruthenium does not find itself in alloy. The surface area of this catalyst is found to increase with ruthenium content.

Among novel procedures, an efficient approach is based on sol–gel technology. Its application to Pt–Ru system was studied in detail in [37]. The basic process is hydrolysis of Pt(II) acetylacetonate and Ru(III) acetylacetonate in acetone medium in presence of tetramethyl ammonium hydroxide. This solution is evaporated up to xerogel formation and later undergoes thermal treatment under controlled atmosphere. The optimized procedure provided powders of high specific surface area (up to approximately 140 $m^2\ g^{-1}$). These powders were characterized in detail by means of XRD, thermogravimetric/differential thermal analysis, scanning electron microscopy (SEM), transmission electron microscopy (TEM), and electrochemical techniques and demonstrated high catalytic activity towards methanol electrooxidation. Sol–gel Pt–Ru technology is still waiting for wider dissemination, but it continues to develop [234].

A general feature of several procedures considered above (including sulphito procedure) is an attainment of high surface areas due to formation of Pt–Ru colloids. A special technique of catalysts preparation with the intermediate synthesis of colloid precursors was proposed by Bonneman and others [235–238] and usually named Bonneman's method. It is based on co-reduction of platinum and ruthenium salts with tetraoctylammonium-triethyl hydroborate in tetrahydrofuran in the presence of surfactant additives for stabilizing colloid particles. It appears to be possible to obtain 1.2-nm size precursor particles of face-centered cubic and multiply twinned decahedral structure. To compare, high temperature decomposition of organometallic cluster $PtRu_5C(CO)_{16}$ used as the precursor results in 1.6-nm mean diameter of particles deposited on carbon black [239].

The properties of catalysts depend on the nature of colloid-support bonding. Colloid precursors were used for catalysts preparation in a number of studies [188, 240–248], and the presence of colloid stabilizers in resulting materials was stressed [243]. Purification of catalysts is a complex problem; it can be solved (at least partly) by adsorbing CO with its subsequent oxidation. The properties of catalysts fabricated by colloid method and by impregnation [174, 249] demonstrated the advantages of the former approach being more suitable for synthesis of polymetallic systems of perfect composition.

Colloid method undergoes further optimization by means of selection of new precursors, reducing agents, stabilizers, solvents, and synthetic conditions. In particular, the reduction of platinum and ruthenium with alcohols in the presence of dodecyldimethyl(3-sulfo-propyl) ammonium hydroxide surfactant (stabilizer) was reported [250]. This technique provides a possibility to control colloid particle size in the range of 2–3.5 nm by means of reaction temperature. The role of subsequent heat treatment is stressed in [245]. The attempts should be mentioned to create highly loaded platinum metal catalysts from colloid precursors [246] or prepared by polyol procedure [219]. In dealing with these catalysts, one should solve the specific problem of complete use of metal. The use of cellulose derivatives [251] favors the stability of nanoparticles.

It is convenient to use the boundary of two immissible liquids for the formation of nanoparticles [252]: Aqueous phase should contain platinum and ruthenium salts, with reducing agent and surfactants for microemulsification being located in organic phase. Triton X-100 and isopropanol were used for the latter purpose [253]. Pt–Ru nanoparticles prepared via microemulsion technique were supported by boron-doped diamond [254]. For this system, no specific effects of the support in methanol electrooxidation were observed, i.e., the role of diamond was limited to collecting current. One cannot exclude higher stability of catalyst on diamond due to high electrochemical inertness of the latter.

Deposition into liquid crystal matrices (known as template deposition) provides comprehensive facilities for Pt–Ru nanostructuring [255, 256], i.e., narrow size distribution of particles with equal space between them, as determined by the wall thickness from the liquid crystal mesophase. Liquid crystals of oligoethyleneoxide were used [256] to template Pt–Ru in the course of salts reduction with metallic zinc. The specific surface areas in the range of 70–80 $m^2\ g^{-1}$ were achieved.

Some surfactants in Pt–Ru deposition solution can probably provide the templating effect as well [257]. Such emulsion and microemulsion systems (in the absence of reducing agent) were used for direct Pt–Ru electrodeposition on recticulated vitreous carbon [258, 259] and resulted in specific surface areas of 12–40 $m^2\ g^{-1}$. Electrodeposition on pressed graphite felts was arranged with adding Triton X-100 to $H_2PtCl_6 + RuCl_3$ solution, with additive concentration high enough to form liquid crystals or micellar structures. In the presence of Triton X-100, more highly dispersed particles and agglomerates in the range of about 10–60 nm were formed under galvanostatic deposition mode, with simultaneous increase of the specific surface area of Pt/Ru (per mass unit). The resulting rates of methanol oxidation at the electrodes prepared in Triton X-100 containing media were higher.

The procedures of Pt–Ru deposition into polymer matrices (polyaniline [260, 261], poly(*o*-aminophenol [262]) were developed, as well as the techniques to prepare metal–polymer composites (in particular, with polycarbozoles [263]).

Sulfide technique proposed by Camara et al. [264] should be mentioned based on using platinum and ruthenium sulfide complexes.

Deposition from vapor phase with subsequent decomposition was described for platinum and ruthenium acetylacetonates [265, 266]. This technique gives homogeneous distribution of particles with approximately 2-nm mean size and narrow size distribution and simultaneously makes it easy to vary metal loading. The activity of catalysts is rather high.

Spray pyrolysis was applied to deposit Pt–Ru on carbon black [267]. Polyethylene glycols of various molecular mass were used at the first stage as co-solvents. It is not quite clear how these additives act, but their presence resulted in the formation of catalysts with improved properties.

One-step technique of Pt–Ru preparation based on flame-spray pyrolisis [268] is of interest. It consists in injection of Pt and Ru precursors dissolved in appropriate solvents through a nozzle, with formation of micrometer-size droplets which burn out in a flame, resulting in metal atoms and/or metal oxide molecules in the gas phase.

One can predict further progress of Pt–Ru deposition from ionic liquids [269–271]. Some attempts were reported for 1-Butyl-3-methylimidazolium tetrafluoroborate solutions with heating in hydrogen atmosphere. Catalysts obtained by these means are at least competitive with E-TEK materials. As the procedure is technologically simple and it is possible to recycle the ionic liquid, some practical prospects should not be excluded. Various types of surfactants were studied [271] as the stabilizers of nanoparticles in ionic liquids, and nonionic surfactants were found to be the most suitable for preparing stable and active catalysts. For reduction, sodium borohydride was used, and surfactants concentration never exceeded the boundary of micelles formation.

When thermal stability of membranes became highly improved (membranes are known now stable above 100 °C, and for some types, the upper boundary approaches 200 °C), the temperature range of catalysts operation had to be widened. It is rather probable that the temperatures above 120–130 °C will be finally the best for practice, especially for automotive applications, as the reaction rates increase with temperature, and noble metal loading can be decreased. However, the longevity of catalyst is crucial [272] because of enhanced segregation and corresponding surface enrichment with Pt affecting catalytic activity.

Electrochemical deposition

Disadvantage of electrocrystallization is less homogeneous distribution of deposit when highly dispersed supports are used. This is the reason of predominating chemical deposition techniques in the area of Pt–Ru fabrication, but Pt–Ru electrodeposits also attract attention. Moreover, these deposits are sometimes considered not as exclusively model systems, but as materials interesting for applications. Classical electrodeposition techniques were applied during two recent decades mostly to predictable preparation of catalysts with certain and variable surface composition. Both potentiostatic and galvanostatic deposition modes are applied, including various pulse modes. The analysis of bulk and surface composition of electrodeposits was accented, as well as comparative testing of electrodeposits and materials of other types.

Several attempts were reported to co-deposit platinum and ruthenium on gold and gas diffusion electrodes consisting of dispersed carbon. The studies [34, 273, 274] are worthy of special comments. In [34], Pt–Ru phase diagram was attracted to interpret asymmetric dependence of electrocatalytic activity towards methanol oxidation on catalyst composition. According to XPS and LEIS data, deposition on gold at 0.05 V (RHE) from $H_2PtCl_6 + RuCl_3$ solution supported by 0.5 M H_2SO_4 resulted in the pronounced enrichment of both micron-thick deposit bulk and (especially) its surface with platinum. Sulfur incorporation was also observed. The authors report the highest activity towards CO oxidation for 50% Ru content, while their deposits most active towards methanol oxidation contained only 7–30% of ruthenium. This difference was discussed in terms of phase separation in the external deposit layers, with further attempt to clarify the role of this factor [275] using ITO-supported alloys. For 40% Ru content, coexisting Pt-rich fcc phase and Ru-rich hcp phase were found to coexist, but this two-phase composition has not affected electrocatalytic behavior.

The problem of segregation was accented in [273], with application of Auger electron spectroscopy (AES) and XPS to surface analysis and parallel use of XRD to determine bulk structure of Pt–Ru deposits on gold, also prepared at 0.05 V (RHE). All deposits were classified as solid substitution solutions of Ru in Pt. Methanol electrooxidation was accompanied by surface restructuring.

Pulse galvanostatic technique was applied in [274], with subsequent XRD, TEM, energy-dispersive X-ray, and AES characterization. Carbon cloth support was preliminary covered with Vulcan XC-72 and polytetrafluoroethylene in isopropanol using ink method. Bulk Pt/Ru ratios in deposition solution and fabricated material appeared to be close. For activity optimization, the delay between pulses was found to be important, and the best samples demonstrated higher activity as compared to commercial catalysts. For these samples, the loading was 2 mg cm^{-2}, with particle sizes in the range of 5–8 nm. The study [274] is of special interest because it confirms competitiveness of electrodeposition and chemical techniques of catalysts fabrication.

More particular studies are listed below. Deposition on gold at 0 V (RHE) from H_2PtCl_6 + $RuCl_3$ solution supported by 1 M $HClO_4$ provided the deposits with Pt surface enrichment (as compared to Pt/Ru ratio in solution), as it followed from XPS [276]. Deposition at the same potential from chloride bath [highly ordered pyrolytic graphite (HOPG) support] is described [277], with XRD and SEM characterization. Unfortunately, electrocatalytic tests in 0.1 M H_3PO_4 were very approximate (arranged under potentiodynamic mode); they led to conclusion of the highest activity for a sample prepared from Pt/Ru=1:1 solution. Deposits with high activity were prepared at 0.05 V in [278] using platinum support and ruthenium nitrosile nitrate solution.

The original technique of Pt–Ru electrodeposition on carbon support was worked out [279, 280]. The mixture of Nafion solution, Vulcan XC-72, and the appropriate amounts of H_2PtCl_6 and $RuCl_3$ were applied over a coarse glassy carbon disc, and pulse galvanostatic deposition was started (assisted by special homemade device providing homogeneity of deposition).

Subsequent and simultaneous deposition of Pt and Ru on HOPG is reported in comparative study [281]. The former two-step route results in multiphase material containing both pure metals and non-stoichiometric ruthenium oxides (oxohydroxides), with a tendency to a fast loss of ruthenium.

The effect of deposition potential and chloride bath composition on the properties of submicron-thick Pt–Ru deposits on gold was revisited in a recent study [35]. The aforementioned factors affect current efficiency, specific surface area, and ageing behavior in both supporting and methanol-containing solutions. Surface enrichment with Pt as compared to deposition solution was also found; it seems to be a general tendency for various bath compositions. The most important conclusion consists in the role of alloying [pure metallic ruthenium cannot be deposited from chloride media at potentials above −0.05 V (RHE)]. The role of Ru-UPD on Au was also stressed. This phenomenon induces the shift of the potential of zero free charge towards less negative values and increases the chloride adsorption being the inhibiting factor for discharge of platinum chloride complexes.

Further studies of Pt–Ru electrodeposition are expected to be turned to more detailed studies of segregation phenomena, optimization of catalysts on real supports, and understanding of the defectiveness effects on Pt–Ru activity, including its evolution in the course of catalysts ageing and training (catalyst stability).

MEA technology

Wide scientific activity around laboratory fuel cells shifted the attention of electrochemists from catalyst preparation to MEA fabrication. MEA consist of proton-exchange membrane (such as Nafion) sandwiched between two porous electrodes whose external sides contact so-called backing layers. The latter are responsible for homogeneous reagent distribution along the electrode surface, products deflection, and current collecting. Most typically, backing layers consist of carbon cloth or carbon paper. The development of MEA resulted in working numerous supplementary materials, namely paste catalysts, catalysts with binders, Nafion solutions, and catalyst inks (suspensions to be applied over membranes). A catalyst ink allows to print, brush, or spray-coat the catalyst into membrane.

When forming electrocatalytic layers, one should take into account various factors, including the size difference of Nafion micelles or agglomerates (about 200 nm) and carbon black particles (about 30 nm) [282]. Catalysts with satisfactory properties can be obtained by modification of Nafion with carbon black and subsequent electrodeposition of Pt–Ru [283]. In frames of this procedure, the properties can be varied by means of deposition potential. Catalyst activity was found to decrease if the size of metal particle became lower than 4 nm.

Some types of MEA are designed by means of membrane impregnation and the subsequent chemical reduction of some precursors, like platinum and ruthenium cationic amino complexes able to take part in ion-exchange processes. Ion-exchange technique with consequent electroreduction [284] provided stable catalysts with high activity. One of the goals of MEA design for DMFC is to prevent methanol crossover. Various aspects of this problem were considered in [285–291].

MEA are used in hydrogen–oxygen fuel cells as well. Their specific features for application in DMFC are as follows: (1) methanol is used in a liquid or vapor form; (2) crossover of methanol; (3) CO_2 should be removed from the layer of anode catalyst and the neighboring backing layer (this can be considered as a problem of CO_2 tolerance). CO_2 accumulation (formation of small bubbles) decreases a total conductivity of the system and induced inhomogeneous potential distribution. Search for some additives is of current importance to improve CO_2 deflection without affecting other characteristics of the device [292].

One fuel cell can contain from a dozen to several thousands of MEA depending on the application. The attempts to optimize the fuel cell as a whole [293–295] take place in parallel with MEA optimization.

One of the most important aspects for MEA construction is the choice of catalyst, attracting attention to comparative studies of catalysts of different genesis. The reported attempts were based on the analysis of literature data [296] or arranged in frames of original studies (of course for a limited group of materials). Among the studies of the second type, we should mention the recent references [297–299]. For comparison of this sort, so-called turnover number was used by some authors, i.e., the number of methanol molecules reacting at one catalytic center per time unit. This approach to comparison of catalysts requires the estimate of the number of active centers per surface area unit, being rather an ambiguous problem for alloys and highly dispersed materials. Less ambiguous consideration is possible for Ru-modified platinum single crystals [299]; it leads to conclusion about the highest turnover number for Ru-modified Pt(100).

The detailed comparison of various Pt–Ru catalysts remains the future problem because of various reasons. First, the majority of catalysts having different prehistory are poorly characterized in terms of surface composition. The second point is the absence of data on true surface areas. Finally, the difference in experimental conditions applied to determine the activity of catalysts provides additional complication. The most important condition is stationarity degree. Comparison of polarization curves measured under cyclic voltammetry mode is the most usual case, and it corresponds to certainly non-steady-state conditions. Indication of time after application of potential step is also insufficient; it is necessary to indicate the independence of current at certain potential on the time passed after step application or some value characterizing current decrease with time.

For basic studies, the catalysts on plane supports (gold, glassy carbon, and HOPG) are the most interesting because of the possibility to apply a wide set of spectroscopic and microscopic techniques to characterize these catalysts. In combination with adatom-modified single crystals and decorated separate nanoparticles, these materials compose a group of model Pt–Ru catalysts which gave birth to a new branch in electrocatalysis. Unfortunately, the supports mentioned above are far from ideality. Nanoparticles on HOPG undergo gradual coalescence, and it is sometimes advantageous to support nanoparticles with less ordered glassy carbon for which coalescence is much slower. Disadvantage of gold support is slow alloying with Pt–Ru nanoparticles, especially for ultrathin catalyst layers and elevated temperatures. The choice of suitable support for the studies of model catalysts imitating the features of real materials remains very important.

Well-characterized Pt–Ru model systems

The majority of studies considered above attracted various physical techniques of materials characterization (mostly ex situ). This approach is not simply typical, but obligatory for electrochemical Pt–Ru studies of the current period. However, the most important advances come from the development of techniques to prepare and study well-defined model Pt–Ru electrocatalysts. It is rather natural that in situ techniques are the most informative in this area. To apply a number of physical techniques operating in vacuum, well-developed ultrahigh vacuum (UHV)-electrochemical systems were used (one of the recent examples can be found in [300]).

Various groups contributed to design and studies of well-defined Pt–Ru systems. Having no idea to belittle their services, we should, however, stress the role of Iwasita-Vielstich [301] team. This team stimulated the arrangement and general direction of Pt–Ru studies, especially at the beginning of the current period. They found in particular that the difference in adsorbed CO bonding energy for linear, bridge, and multibonded forms are not dramatic. They made a pioneering attempt of Fourier transform IR (FTIR) study in the course of methanol oxidation on Pt–Ru [302]. It is difficult to underestimate the role of differential electrochemical mass spectroscopy (DEMS) [303] and electrochemical thermal desorption mass spectroscopy [304] studies of methanol oxidation products. These papers also returned us to reconsideration of the role of electronic factors (or ligand effect), these basic ideas preventing the limited appreciation of Pt–Ru electrocatalysis in terms of bifunctional mechanism exclusively.

The necessity to work with well-defined catalysts for understanding the nature of processes in Pt–Ru system was clearly demonstrated by Berkeley group (Gasteiger, Markovic, Ross, and Cairns) [305–309]. They mentioned a crucial weak spot of the previous studies, namely the absence of direct data on the presence of oxidized Ru at the surface and the ratio of oxidized and metallic Ru, as well as the data on true surface areas and surface elemental composition related just to operating conditions. The latter is of special importance in the context of parallel development of knowledge on surface segregation [310]. Pt–Ru is a classical example of surface segregation of the element with lower heat of sublimation [305, 311]. Adsorption of CO as a test molecule attracted the main attention, as it gave a tool to discover some delicate details of catalyst electronic structure [307].

Well-characterized ruthenium electrode

The first study of Ru electrode under CO oxidation conditions was published by Leung and Weaver [312] who applied surface-enhanced Raman spectroscopy (SERS) technique. A novel SERS strategy was later proposed by Chan et al. [313] with the use of ultrathin layers of platinum group metals on gold support giving a possibility to obtain the vibrational spectra of oxospecies monolayers with high sensitivity under both electrochemical and gas-phase conditions. Potential-dependent SER spectra related to electrochemical Ru oxidation were compared to temperature-dependent SER spectra for thermal Ru oxidation and found complete reduction of Ru to metal only under polarization in hydrogen evolution region. A simple technique of Au surface modification with nanoparticles of platinum group metals (including Pt–Ru) was worked out in [314], with subsequent registration of electrochemical responses and infrared reflection absorption spectroscopy spectra.

Ertl and others [315–317] managed to study the single crystalline Ru surfaces in UHV-EC system, with a possibility to apply LEED, reflection high-energy electron diffraction, and AES in combination with cyclic voltammetry. The ordered (2x2)-O layers on Ru(0001) were observed already in the hydrogen region, and the activity of these layers towards CO oxidation was documented. On the basis of FTIR data, the authors concluded the formation of CO islands and assumed that oxidation occurs at the boundaries between the islands of adsorbed CO and oxygen adatom domains. Weakening of CO surface bonding with potential shifted towards more positive values (and simultaneous increase of oxygen adsorption) was found. Linear form of adsorbed CO and threefold-hollow binding adsorbate were found at Ru(0001) surface, while only linear form was observed at polycrystalline Ru.

In situ FTIR was applied to study CO adsorption on nanometer-thick ruthenium films electrochemically deposited on glassy carbon [318]. These films were also characterized by scanning tunneling microscopy (STM). Some difference of adsorbed CO spectra (as compared to similar spectra for polycrystalline ruthenium [319, 320]) was explained by specific features of nanostructures. Zheng et al. [321] studied nanometer-thick layers of Pt–Ru alloy and concluded the specific features of their IR spectra and high activity towards CO oxidation.

Data for Ru/Au(111) system are of interest to understand the properties of Ru adatoms, as the properties of this system are governed purely by ruthenium. Au does not induce any bifunctionality, being completely inactive towards CO adsorption at potentials below 1 V (RHE). However, the studies of this system are complicated by Au (111) surface reconstruction starting at certain potential and inducing the formation of periodic dislocation network. The consequence of this phenomenon was studies by Strbac et al. [322]. According to in situ STM, Ru submonolayers consist of islands (1–2 nm in diameter) which nucleate at the specific sites of reconstructed surface (elbows, fcc areas). At higher coverage, the islands coalesce and form highly defective monolayer, most probably having pseudo morphic lattice. Multilayer growth is accompanied by appearance of significant surface roughness. Ru/Au(111) oxidation is similar to oxidation of bulk Ru. CO forms irreversibly adsorbed layers on Ru deposits and suppresses oxygen adsorption. At low ruthenium coverage, one can observe two CO desorption peaks assigned to CO adsorbed at Ru islands and at island edges, while only one peak appears at high Ru surface coverage or on multilayer deposits. Potential of CO oxidation onset is more positive for Ru (sub)monolayers than for bulk Ru. This can be explained by the increase in CO adsorption energy resulting from electronic modification of Ru layer (Au-induced pseudomorphism, which can be considered as strain effect).

Decorated Pt–Ru$_{ad}$ materials

Ru-modified platinum single-crystalline electrodes and nanoparticles attracted enormous attention. These catalysts abbreviated as Pt–Ru$_{ad}$ are also named “decorated”. Decoration is available via electrochemical treatment or spontaneous deposition techniques using various solutions of ruthenium precursors as well as by means of Ru sputtering or vapor phase deposition [323–345]. A special role of decorated systems was stressed by Wieckowski who considers decoration of single crystals as a special type of templating. Actually, the structure of adlayer and atomic ratio of surface components can be easily controlled, as both are governed by deposition conditions. In addition, adatoms diffusion along the surface and into catalyst bulk can hardly be pronounced at ambient temperatures. As Ru adatoms can be easily desorbed under anodic polarization, there are no problems to renew the surface.

Spontaneous deposition takes place from aged RuCl$_3$ solutions in perchloric acid [299, 346]. This process is assumed to take place due to co-adsorption with anions. Then, deposited ruthenium species are reduced electrochemically, resulting in strongly bonded ruthenium (being mostly in metallic state) and anions desorption. According to AES and STM data [347], the highest surface coverage attained in the course of one procedure of this sort is approximately 20%. Thus, obtained catalysts demonstrate the pronounced activity towards methanol oxidation [330]. Ru adlayer at Pt(111) was found to be more active methanol oxidation catalyst at low potentials as compared to Os adlayer at the same surface [348].

Decorated catalysts were used for understanding the role of electronic factors in electrocatalysis. In connection with this problem, Wieckowski's group developed electrochemical nuclear magnetic resonance (EC-NMR), a strong experimental technique sensitive to electronic structure of metals, including adsorbate-modified systems. The technique was applied [349–351] to clarify the promotion mechanism in Pt–Ru system. Pt–Ru catalyst was presented by commercial platinum black (particle size of about 10 nm) modified by spontaneous deposition from $RuCl_3$ aqueous solution. It was demonstrated that modification results in the formation of monoatomic Ru islands. CO domains were found at both platinum and platinum–ruthenium regions, with the pronounced Ru effect on electronic dynamic effects in both types of domains.

Formation of CO domains is unusual phenomenon, as CO species tend to repulsion. It was assumed that the specific features of water adsorbed on platinum and ruthenium and water interaction with CO results in islands formation despite repulsion.

Electronic alterations caused by Ru in Pt–Ru alloy nanoparticles were studied in more detail using ^{195}Pt- and ^{13}C-EC-NMR and commercial materials [352]. The enrichment of nanoparticle surface with Pt was found, and the increase of the number of Pt d-band vacancies in Pt–Ru alloy was concluded, in agreement with ligand effect hypothesis explaining Pt–Ru electrocatalysis. At the same time, IR study [353] supported mostly bifunctional mechanism. Correspondingly, both mechanisms should be further considered.

Any quantitative estimate of contributions of these effects can hardly be unambiguous. According to [343], only a minor portion (about 40 mV) of a total CO overvoltage decrease induced by Ru addition (about 170–250 mV) can be induced by ligand effect. Similar conclusions were presented earlier in [339].

A number of model Pt–Ru systems were studied by means of XPS analysis in EC-UHV configuration using nanoparticles immobilization on Au support [354]. All bimetallic particles in reduced state were more active towards methanol oxidation than partly or completely oxidized particles. The activity decreases is a sequence Ru-on-Pt > Pt–Ru alloy > Pt-on-Ru. This result was interpreted in terms of strong dependence of surface electronic state on mutual location of Pt and Ru atoms.

Davies et al. [336, 338] published detailed study of Pt (100) modified by Ru sputtering with subsequent heating at various temperatures. The behavior of thus obtained electrodes was demonstrated to depend strongly on the presence of Ru in adsorbed or incorporated (through annealing) state, in particular on its location in the top layer or in the second/third layer of Pt. Ru top layer demonstrated better promotion of CO oxidation, while Ru in deeper layers never affected this process.

Several platinum modification with ruthenium procedures were developed by Bergens and others [355–358]. One of these procedures is based on the hydrogenation of $Ru(COD)(\eta^3\text{–}C_3H_5)_2$ in hexane in the presence of Pt, arranged under mild conditions, while Ru is deposited on Pt, and cyclooctane and propane are formed. More convenient procedure (despite that it requires more sharp reduction conditions) involves $Ru_4H_4(CO)_{12}$ precursor. It can be considered as self-limiting, as the reduction stops after attaining a certain surface coverage with Ru, and the rest part of surface appears to be poisoned by CO. To obtain higher Ru coverage, one should repeat the procedure after oxidation of CO, and anytime the increase of coverage is the same, so catalysts with a definite degree of modification can be prepared. Similar technique can be arranged with the use of $RuCl_3$ precursor by means of saturating platinum nanoparticles with hydrogen before each modification step. However, the authors do not exclude that their procedures can result in 3D structures, not exclusively 2D.

Synthesis of novel ruthenium compounds was accompanied by attempts to use them for modification of platinum nanoparticles to design the efficient catalysts. In particular, adsorption of ruthenium tetramethylcyclam 14 and 15 on carbon-supported platinum [359] resulted in catalysts with activity close to activity of commercial samples at low potentials.

To study the promotion mechanism for Ru-modified Pt single crystals, Friedrich et al. [360] covered Pt(111) with Ru islands or Ru atoms deposited at the central part of the surface. These samples were characterized by STM, and CO adsorption was addressed in IR spectroscopic experiments. Surface diffusion of CO species was documented, and the lower limit of surface diffusion coefficient $D_{CO} > 4 \times 10^{-14}$ cm^2 s^{-1} was estimated. The importance of CO mobility for interpretation of electrocatalytic behavior of Pt–Ru is also stressed in theoretical study of Koper et al. [361] who mentioned a crucial role of mixing of Pt and Ru atoms for satisfactory mobility. The relatively low activation energy of diffusion process was concluded in [362].

For clarification of platinum and ruthenium atoms distribution along the surface, the IR spectra of adsorbed CO are rather informative. If these atoms mixed at atomic level, a single band is observed, with characteristic frequency between the frequencies of linear CO adsorbed on pure Pt and Ru, respectively [363]. If Ru clusters are formed, one can expect at least two or even three extended bands, as it was observed experimentally in [326, 331] for catalyst electrodeposited on Pt(111). These bands were assigned to CO on Ru islands, Pt support, and Pt–Ru boundary regions (banks).

Massong et al. [364] compared the electrocatalytic properties of Ru-decorated Pt(111) and Pt(332). Oxidation of adsorbed CO manifested itself either by double peak or by a shoulder of a complex shape after the major peak. Taking into account Monte Carlo simulation results, the authors interpreted this bifurcation in terms of slow CO surface diffusion towards Ru sites at the surface. It is interesting to note that the main peak observed at Ru–Pt(332) appeared at less positive potentials as compared to desorption peak for Ru-modified basic Pt(111) plane.

Well-characterized Ru–Pt$_{ad}$ system

Another type of model systems was proposed and studied in detail by Brookhaven group. Brankovich et al. [365] discovered spontaneous deposition of Pt on Ru(0001) pretreated in UHV. Mechanism of this phenomenon demonstrates some difference from spontaneous and electrochemical deposition of ruthenium on platinum and probably can be explained in terms of local galvanic cells. Spontaneous platinum deposition takes place only on freshly prepared metallic surface and fails at the oxidized surface. It was applied to modification of Ru(0001), $\mathrm{Ru}\left(10\overline{1}0\right)$ and carbon-supported Ru nanoparticles (on Vulcan XC-72). Thus, prepared catalysts were studied by means of X-ray scattering, STM, FTIRS, and high-resolution TEM techniques [366]. The dramatic difference in the behavior of Ru(0001) and $\mathrm{Ru}\left(10\overline{1}0\right)$ in sulfuric acid solutions confirmed a high structural sensitivity of interfacial processes. For Ru(0001), a single anodic peak at approximately 0.6 V (RHE) is assigned to one electron oxidation of ruthenium. For $\mathrm{Ru}\left(10\overline{1}0\right)$, two rather reversible peaks at 0.12 and 0.3 V appeared, looking similar to peaks of hydrogen desorption on platinum. However, with taking into account CO replacement data, the authors attributed these peaks to partial ruthenium oxidation. Similar peak at 0.1 V with consequent shoulder appeared on Ru(0001) as well in perchloric acid solution [367]. Such a difference of Ru(0001) behavior in sulfuric and perchloric media was explained by strong structural sensitivity of bisulfate anions adsorption studied later in [368]. Later, the technique of CO charge displacement was applied [369] to clarify the details of Ru(0001) behavior in perchloric solutions.

Adzic and McBreen observed monolayer-to-multilayer transition in the course of Ru(0001) decoration with platinum. Finally, they obtained the ordered array of columnar platinum particles (3- to 5-nm height and diameter, with 6- to 10-nm distances between the particles, as it follows from STM visualization). Platinum decoration was applied to ruthenium nanoparticles supported by Vulcan XC-72. Metallic nanoparticles on carbon were of cuboctahedron icosahedron shape, and platinum formed 2D islands on their surface. Decorated catalyst demonstrated much higher CO tolerance in hydrogen mixed with 100 ppm CO as compared to E-TEK catalysts despite higher content of noble metals in the latter. The authors attributed this effect to modification of electronic properties of the surface metal layers induced by the presence of Pt, not to bifunctional mechanism. Later, the catalyst prepared by spontaneous deposition of platinum on ruthenium nanoparticles was used to study the kinetics of hydrogen anodic oxidation in CO-free and CO-contaminated systems [370].

The properties of Pt-decorated ruthenium and commercial Pt–Ru catalyst were compared [371] in relation to methanol oxidation at 130 °C using a cell with Nafion membrane operating as electrolyte. To prepare decorated catalyst, amorphous ruthenium oxide was impregnated with diluted H_2PtCl_6 solution and reduced in hydrogen gas. Final material with ultra low loading of approximately 0.1 mg cm^{-2} demonstrated the activity only 35% lower than commercial E-TEK catalyst with 2 mg cm^{-2} loading. This result, in combination with the findings of Bergens and others [355–358], demonstrates real practical prospects of decorated materials.

Finally, we should mention that using high-resolution SEM, Knutson and Smyrl [372] were able to observe directly the pores of 2- to 4-nm diameter in electrodeposited Pt–Ru nanoparticles. The existence of these pores is responsible for the high surface area of these particles and most probably the other properties.

The studies of well-defined model systems contributed to advanced understanding of the role of a number of factors essential to explain synergetic effects and mechanisms of electrocatalysis at Pt–Ru surfaces despite the absence of exact agreement of all results and conclusions.

The nature of electrocatalytically active ruthenium species

Attributing of the unique electrocatalytic activity of Pt–Ru to metallic or oxidized ruthenium was widely discussed long before the appearance of technical tool to control ruthenium oxidation state at the surface. As ruthenium is easily oxidized, it looked rather natural to assume that some oxo- or oxohydroxo species are responsible for the promotion of methanol oxidation. Later, some authors [85, 90, 373–377] mentioned a special role of oxidized ruthenium forms on the basis of XPS and Moessbauer spectroscopy data confirming the presence of ruthenium oxohydroxides in Pt–Ru alloys.

Recently, this problem arose rather lively discussion stimulated by Rolison group publications [378, 379]. According to these papers, a catalyst containing hydrated ruthenium oxide RuO_xH_y is several orders of magnitude more active as compared to purely metallic Pt–Ru. The authors had some doubts concerning previous interpretation of XRD results as unambiguous evidence of oxide-free catalyst composition, as XRD is restrictedly suitable for phase analysis of highly dispersed materials. However, XPS studies [380] demonstrated complete electrochemical reduction of the electrode material initially containing RuO_2 nanoparticles, in agreement with ellipsometry and electrochemical quartz crystal microbalance (EQCM) results [325, 381] on complete oxide reduction under fuel cell operating conditions. The same was concluded [382] from in situ X-ray absorption near edge structure data: Only metallic state of Pt and Ru was found under H_2 and H_2 + CO atmosphere. According to [383, 384], a catalyst consisting of metallic components is more active than a catalyst containing oxidized ruthenium species. The presence of RuO_x is desirable because of another reason: It increases the proton conductivity of catalytic layer. Probably, this is just the reason of high activity observed for Pt–RuO_x [385]. The increase in activity of commercial Johnson–Matthey catalyst after its reduction under hydrogen gas confirms the decisive role of metallic ruthenium. Let us also mention the studies [386–391] demonstrating no convincing evidence of the necessity to have oxidized ruthenium species for attaining high catalytic activity of Pt–Ru. Lasch et al. [388] found no difference of well-crystallized and amorphous catalysts (the latter are usually consist of hydrated ruthenium oxides).

Recently, MacDougall and coworkers [392, 393] tried to clarify the nature of active ruthenium species using the approach of Lasch et al. [387, 388] by studying a series of catalysts with artificially added ruthenium oxides. They applied various physical techniques to catalysts characterization and studied the kinetics of CO and methanol oxidation. The authors concluded higher activity of alloys as compared to mixed catalysts. They also mentioned that if methanol concentration exceeds 0.1 M, no oxidized ruthenium species is observed in potential region being of interest for applications. It seems like ruthenium oxides are reduced under this polarization mode, and the presence of platinum can support this process by providing active hydrogen species. This is probably the reason of high activity demonstrated by RuO_x*H_2O loaded with platinum nanoparticles [391].

Optimal Pt/Ru ratio and size effects

The problem of Pt/Ru ratio optimization in Pt–Ru catalyst requires special discussion. As it was already mentioned above, the ratio corresponding to the highest activity depends on the reaction type (CO or methanol oxidation) and the catalyst type (electrodeposited, supported, or unsupported Pt–Ru). The reasons of disagreements are still not clear. The model proposed in [306] assumed the necessity of threefold Pt positions in the vicinity of Ru atom; however, it was not reconsidered systematically with taking into account the formation of ruthenium islands. Not only is the total Pt/Ru ratio important, but also the mutual location of Pt and Ru atoms. Namely, the activity of catalysts fabricated by metals co-deposition and subsequent deposition of Pt and Ru layers appears to be different [394].

More evident tendency is observed for temperature dependence of the optimal ratio: The majority of authors agree that for methanol electrooxidation, the higher is the temperature, the higher should be the ruthenium content. One of the reasons is methanol adsorption on Ru atoms as well at elevated temperature [309]. Under these circumstances, Ru already do not work as OH species supplier. Optimal composition also depends on operating potential: Catalysts with higher ruthenium content are more active at lower potentials and become less active with increasing potential because of easier ruthenium oxidation and appearance of inactive ruthenium species. There are also no doubts concerning the optimal ratio dependence on electrolyte composition because of negative shift of the potential of zero free charge with the increase in Ru content and corresponding increase of anions adsorption at low potentials. Unfortunately, no data exist related to potentials of zero charge in metal/polymer electrolyte systems, and the comparison of Pt–Ru behavior in aqueous solutions and in polymer electrolytes remains actual.

Size effects are actively discussed. Optimal size is typically considered to be 2–3 nm [31]. Watanabe et al. [395] declaim the existence of size effect at least for particles diameter exceeding 1.4 nm and consider size effects reported by other authors as less reliable because another important factor, namely the distance between neighbor particles, was not controlled or taken into account.

Gradual changes of particle size in the course of catalyst operation were mentioned in many papers even for relatively short experimental tests. It should be mentioned that sometimes, the activity of catalyst appeared to improve with operation time, and some initially less active samples finally demonstrated the best characteristics despite particle size increase. A slight decrease of activity with aging time was observed for electrodeposited Pt–Ru [35]. Actually, the clarification of the existence and sign of size effect requires further studies.

Further development of knowledge related to the role of structural factors, size effects, and the oxidation state of Ru in Pt–Ru electrocatalysis is presented in the recent papers [396, 397].

Real surface area determination

Any correct comparison of catalytic activity for different Pt–Ru materials is impossible in the absence of true surface area data.

In early studies [17, 20], Brunauer–Emmett–Teller (BET) technique was applied to determine true surface area, and these data were compared with coulometric results for “hydrogen adsorption” region obtained by means of chronopotentiometry (charging curves) or voltammetry. The potential regions were found for which the agreement of BET and coulometry data took place. The problems arose from the overlap of hydrogen and oxygen adsorption regions (being stronger for higher ruthenium content). This overlap prevented any straightforward application of traditional H-UPD technique of surface area determination. BET is also applied in modern studies of Pt–Ru. For supported Pt–Ru particles, one can also determine true surface area using selective gas titration [398].

The most usual electrochemical techniques to estimate Pt–Ru surface area are currently based on foreign metal adatoms, especially copper [399]. This approach is extremely useful for carbon-supported catalysts, as adatoms can be formed only on metallic portion of complex surface. The choice of copper goes from close atomic radii [0.128 (Cu), 0.138 (Pt), and 0.134 (Ru) nm] and convenient potential region of Cu desorption at relatively low potentials, making it easy to introduce correction for double-layer charging and oxygen adsorption.

Another electrochemical technique, also widely applied, is CO stripping voltammetry [309, 400–402]. Basically, this technique gives a chance of separate determination of “platinum” and “ruthenium” portions of true surface area, as desorption from Pt and Ru takes place at different potentials. However, a strong overlap of two peaks is usual for real materials. Some complications can be avoided if DEMS [403] or IR spectroscopy [404] are applied in parallel with registration of stripping charge.

The problem of the true surface area determination for supported and unsupported Pt–Ru was discussed in detail by Green and Kucernak [405] who compared CO stripping and Cu-UPD techniques and concluded that the latter is more reliable. Combination of these techniques gives an opportunity to find the total true surface area of alloy. Cu-UPD also provides information on surface elemental composition and the ratio of surface Ru sites existing in oxidized and metallic states (no Cu-UPD takes place on oxidized Ru). A number of additional problems arising when one determines the real surface area using various adsorbates were stressed recently in [406].

Measuring the rate of oxalic acid oxidation was also discussed in relation to Pt–Ru surface area determination [407]. Platinum is active towards this process at low potentials, while Ru starts to be active only at higher potentials. Assuming the absence of synergetic effects, one can try to separate “platinum” portion of the surface area. In combination with CO stripping, this technique can be considered as rather useful.

Gilman and others [408, 409] applied fractal treatment of STM images to determination of Pt–Ru surface areas. This technique provides some reasonable results for electrodes of low roughness.

Ru crossover

Testing of model fuel cells with PEM revealed Ru crossover phenomenon consisting in ruthenium dissolution from DMFC anode, diffusion of dissolved species through membrane, and Ru deposition at DMFC cathode. Crossover problem was formulated by Piela et la. [410] and studied in [411–414]. Some authors mentioned low Nafion stability in methanol-containing solutions. Crossover tends to enhance with operating time, and newly deposited ruthenium damages the cathode performance in relation to oxygen reduction, with parallel destruction of polyelectrolyte membrane.

The nature of crossover is still far from being clear. According to Pourbaix diagram, ruthenium is expected to be thermodynamically stable in the potential range of DMFC anode operation. EQCM study of ruthenium deposits on gold [415] confirmed that slow dissolution takes place at potentials below 1 V (RHE). This process should become slower for alloys. No ruthenium dissolution from alloys was found for samples on platinum and gold supports up to 0.8 V RHE [35]. For these model electrodeposited materials [35], degradation manifested itself only by Ru diffusion into catalyst bulk. This is why one can conclude the important role of carbon support nature and/or PEM functional groups in ruthenium dissolution enhancement. Actually, crossover can be predicted, taking into account the data on disintegration of some types of carbon-supported Pt–Ru materials in alcohol-containing solutions (see above).

To prevent the crossover, carbon-supported catalysts modified with nanostructured ruthenium oxide were prepared [416]. Platinum electrode protected with crystalline ruthenium acid $H_{0.2}RuO_{2.1}*H_2O$ (proton conductor) appeared to be stable and effective for methanol and CO oxidation.

One of the most recent catalyst and membrane degradation studies was reported in [417]. Extremely complex processes with participation of perfluorosulfonic acid electrolyte in PEM FC follow from a recent paper [418].

CO tolerance of Pt–Ru system

CO tolerance of Pt–Ru attracted attention already at the initial period of the studies of this system. During the current period, this problem was actively addressed in terms of tolerance mechanisms, and CO tolerance was considered as one of the most important parameters taken into account for Pt–Ru optimization [80, 311, 419–427]. Some aspects were reviewed by Conway and Tilak [428].

Tolerance in a wide sense is considered as the decrease of poisoning CO effect on methanol electrooxidation as well as still high rate of hydrogen ionization in the presence of CO contamination. We discuss tolerance below just in the context of reformate gas oxidation. Under these circumstances, tolerance can be characterized by two parameters: so-called ignition potential (corresponding to the beginning of sharp current growth when oxidizing H_2 + CO mixture, with subsequent approaching the diffusion limit) and the values of oxidation current corresponding to vicinity of equilibrium potential. Ignition potential corresponds to the onset of CO oxidation and the release of some surface fragments previously poisoned with CO. The initial region of polarization curve characterizes the reaction kinetics at the surface poisoned with CO. General view can be constructed from the data on CO-selective oxidation from reformate, oxidation of CO dissolved in electrolyte solution in the absence of hydrogen, and oxidation of hydrogen in the absence of CO. Useful tolerance criterion can follow from impedance spectroscopy [426], consisting in transition to pseudo-inductive behavior of system.

Kinetic scheme representing tolerance [429] takes into account the presence of both linear and bridge forms of adsorbed CO, as well as the linear forms of COOH and CHO, under assumption of the easiest oxidation of bridge CO. To clarify tolerance nature, EC-NMR data [349] are of special importance, which give evidence of weaker CO bonding in presence of ruthenium.

Catalyst optimization as related to tolerance parameter (considered for H_2 + CO mixtures) included a search for some additives to Pt–Ru improving this parameter. Namely, tolerance was found to increase when Mo, Nb, or Ta were incorporated into carbon-supported Pt–Ru [421], and Mo was reported as the most efficient. A study of filtering RuO_xH_y/C layer as a tool to tune Pt–Ru tolerance was also reported [422].

Systematic studies of Pt–Ru tolerance optimization were published by Fenton and others [423–425] who indicated an additional factor increasing the activity of poisoned catalyst: Reactions of CO with hydrogen (and probably with water molecules) at low potentials can be activated to a certain degree at various catalysts. These reactions can result in the release of a portion of unpoisoned surface or in formation of weakly bonded species replaced with hydrogen. Some additional information about these processes can result from the studies of adsorbed CO replacement with dissolved CO arranged with the use of ^{14}C tracer [430]. The effect of H_2O_2 additives on the tolerance of PtRu anode was studied in [431]. The research concentrated around fabrication of CO-tolerant anodes was published recently [432].

Mechanism of methanol and CO electrooxidation on Pt–Ru

Mechanistic aspects of electrocatalytic processes on Pt–Ru catalysts of different genesis were (to some extent) touched in a large number of works. For methanol oxidation, the most usual approach assumes the existence of two parallel pathways (dual-way mechanism), as it was clearly formulated for Pt electrode by Breiter [433]. For platinized platinum, a scheme with up to four parallel pathways was proposed [434]. It was also assumed that the intermediates of one of the routs can be transformed into intermediates of some other routs [435]. The most simplified version of this scheme looks as follows [436]:

$$\begin{tikzcd}
 & \mathrm{RI} \arrow[dr, "2"] \arrow[dd, "3"] & \\
C_1 \arrow[ur, "1"] \arrow[dr, "4"'] & & CO_2 \\
 & \mathrm{P} \arrow[ur, "5"'] &
\end{tikzcd}$$

where RI is the reactive intermediate, and P is poisoning intermediate. The most difficult aspects consist in determining RI nature and proving the existence of rout 3.

The structural data for model catalysts, various in situ results on CO and methanol adsorption and on electrooxidation products composition (especially obtained by spectroscopic techniques) are actively involved now in the formulation of specified mechanisms. Novel approach to this problem is based on constructing polarization curves from the data on current efficiency of certain products, with simultaneous allowance for certain surface coverage with adsorbates. It is important that for low temperatures, one can ignore methanol adsorption on ruthenium sites, while CO is easily adsorbed on both Pt and Ru.

Potentiostatic current transients provide useful information. This technique was widely applied to study the oxidation of adsorbed species [175, 176, 276, 303, 323, 340, 437, 438]. Current transients of pre-adsorbed CO oxidation are asymmetric, with a broad descending branch and potential-dependent time/current at a maximum. An attempt to model these curves in terms of potential-dependent nucleation and growth of islands formed by oxygen-containing species was reported [276]. This model assumes the absence of surface diffusion of both CO and OH adsorbates. However, according to [361], the surface diffusion can be hardly ignored. Moreover, synergetic effect in Pt–Ru system found no explanation if surface diffusion is not considered. More detailed analysis published by Jiang and Kucernak [438] led to satisfactory agreement with a model of 2D nucleation and growth of islands accompanied by 2D surface diffusion. Islands are supposed to be formed by CO-free surface regions available for adsorption of adsorbed OH and water. The attempts to model current transients for methanol oxidation lead to more complex and ambiguous schemes.

Temperature effects of both methanol [439, 440] and CO [441, 442] oxidation were recently reexamined. The values of activation energy determined by different authors demonstrate no quantitative agreement, which is a not surprising fact because of the difference in experimental conditions and types of catalysts. All reported values are high enough to exclude diffusion control; however, more detailed interpretation is hardly possible.

Impedance spectroscopy was applied to study electrooxidation mechanisms [443–445] and resulted in the appearance of some equivalent schemes, while any principal results of this technique remain future expectation.

The most evident prospects of progress in understanding mechanistic aspects are connected with online product analysis at various potentials. Some attempts of this sort are known from the earlier studies. Most important results are published in [446–449]. Iwasita's group actively contributed to the studies of methanol electrooxidation using various techniques and, in particular, dealing with analysis of products [450–453]. Despite that the majority of these data are obtained for platinum, including single-crystalline platinum electrodes, they can be (with a number of reservations) applied to Pt–Ru system. Recently, the oxidation of formaldehyde was studied on PtRu catalysts of various compositions [454]. Oxidation products usually contain formic acid and formaldehyde, and the aforementioned citations suggest not only parallel routs of these products formation

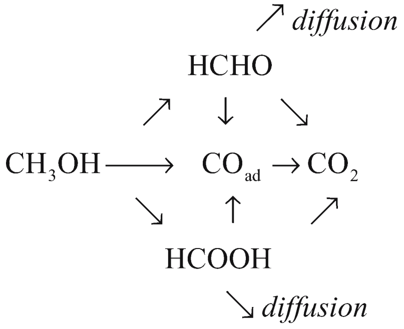

but also different mechanisms. Langmuir–Hinshelwood mechanism is proposed for oxidation with CO_2 formation, while formation of less-oxidized stable species is attributed to Eley–Rideal mechanism. The formation of the latter products on Pt(111) was interpreted as the consequence of methanol adsorption via oxygen atom, with formation of methoxide species H_3CO at the first stage of adsorption. Sulfate anion was found to affect strongly the reaction rate and the ratio of various pathways.

Wang et al. [449] stated different dependencies of partial pathway rates on methanol concentration: At low potentials, the pathway with formation of adsorbed CO is concentration-independent, while the pathways leading to HCHO and HCOOH depend on this parameter. According to recent study [455], the quantity of intermediate formaldehyde species is lower on Pt–Ru as compared to Pt.

Classical approach to study reaction mechanism using Tafel slope and reaction order was applied in [456, 457]. However, as conclusions are based on analysis of non-steady-state polarization curves, it is difficult to use it for mechanism formulation.

Novel modification of DEMS technique [458] was applied to study mechanistic aspects with the use of commercial catalyst at the MEA interface. The results agree with previously obtained for simpler model systems. In particular, CO is found to be predominating adsorbate, but it is still unclear whether it is intermediate or poison. Let us remind the early data of the first period of Pt–Ru studies: The rates of chemosorbed and dissolved methanol oxidation were found to be close, but not equal, so some contribution from weakly bonded organic species could not be ignored (at least at low potentials and temperatures). Unfortunately, the nature of weakly bonded species remains unknown despite numerous attempts to discover it.

The data on radioactive CO exchange on Pt–Ru [430] are of great interest and should be developed in future. Lei et al. [459] tried to clarify the role of C–H bonds activation in methanol using deuterated water and acid and found that this factor affects methanol oxidation rate, at least inside a certain range of potentials. These data are most probably related (at least to some extent) to slow methanol adsorption.

As it was stressed in the first part of this review, the important mechanistic criteria go from pH dependence of the reaction rate at constant overvoltage and also from the Tafel slope. The latter are mentioned in a number of papers cited in this section (unfortunately, they are most usually related to non-steady-state conditions and uncertain overvoltage values). As it is stressed in [460], for optimized catalysts, the slope of 64 mV per current decade can be observed at low overvoltage and temperature of about 70 °C. This slope corresponds to slow organic adsorbate interaction with adsorbed OH specie.

A scheme of methanol electrooxidation on Pt proposed in [31] takes into account the surface geometry, the specific sites for certain adsorbed species, and their migration routs. This scheme induced a number of critical notes and can be hardly applied immediately to Pt–Ru. The progress in the area is expected from new experimental studies and parallel development of computational/model approaches.

At the same time, rather simple schemes going from formal kinetics already found application to modeling the processes at DMFC anodes and even operation of fuel cell as a total [461–465]. These schemes take into account two types of surface sites (Pt and Ru, two-site mechanism) and assume the consequent reactions of methanol adsorption, one-step formation of adsorbed CO, and its oxidation with adsorbed OH formed reversibly from water:

$$\mathrm{CH_3OH} \underset{k_1'}{\overset{k_1}{\rightleftarrows}} \mathrm{CH_3OH_{ad}}$$

$$\mathrm{CH_3OH_{ad}} \xrightarrow{k_2} \mathrm{CO_{ad}} + 4\mathrm{H}^+ + 4e$$

$$\mathrm{H_2O} \underset{k_{3,1}'}{\overset{k_{3,1}}{\rightleftarrows}} \mathrm{OH_{ad,Pt}} + \mathrm{H}^+ + e$$

$$\mathrm{H_2O} \underset{k_{3,2}'}{\overset{k_{3,2}}{\rightleftarrows}} \mathrm{OH_{ad,Ru}} + \mathrm{H}^+ + e$$

$$\mathrm{CO_{ad}} + (\mathrm{OH_{ad,Pt}} + \mathrm{OH_{ad,Ru}}) \xrightarrow[k_{4,1}']{k_{4,1}} \mathrm{CO_2} + \mathrm{H}^+ + e$$

One of the last papers in this area published by Shivhare et al. [466] contains a brief analysis of all previous modeling attempts. Currently, developing simplified models explain the effects of methanol concentration and temperature, but still were not verified in more detail. A simplified scheme named Kauranen–Scou–Munk model [461] was used recently in [467].

Unfortunately, no analysis of pH effects was reported in frames of these models. Possibility of several parallel routs also was not considered. A high number of fitting parameters (rate constants) corresponding to schemes under discussion complicates application of model relations. The involvement of electrochemical step (second reaction in the scheme) requires special discussion. In general, consideration in terms of formal kinetics roughly (qualitatively to a great extent) agrees with experimental data, but only for the region of higher potentials.

Environmental aspects of Pt–Ru system

Wide-scale practical applications of DMFC meet a number of ecological and health requirements. As it follows from discussion given above, Pt–Ru is a highly efficient catalyst to oxidize methanol to CO_2. However, under some modes, formic acid, formaldehyde, methyl formate, and methylal appear to be predominating products [468–471]. There is no clarity with the reasons; probably, methanol molecular orientation in reaction layer plays a role, as was mentioned in [472]. To solve environmental problems, further studies of methanol adsorption and the nature of intermediate species are highly desirable.

One should not forget that methanol itself is a dangerous substance with rather high vapor pressure. This fact induces new and new search for alternative fuels.

Pt–Ru system for other fuels

A lot of papers consider Pt–Ru as a catalyst for electrooxidation of organic substances as possible future fuels used instead of methanol. The most studied candidates are ethanol, ethylene glycol, propanol isomers, dimethyl ether, trimethoxymethane, dimethoxymethane, trioxane, ethylal, and dioxalane.

Ethanol induces a special interest, being the recycled fuel currently used in some countries (for example, Brasil) in combustion engines. Ethanol itself and its oxidation products are less toxic as compared to methanol and the products listed in the previous section. Finally, ethanol crossover is less pronounced due to its larger molecular size. The latter factor is crucial for choice of alternative fuels. The enhanced Pt–Ru activity towards ethanol oxidation was demonstrated already in the course of initial studies, despite synergetic effect being less pronounced than for methanol. Some doubts concerning Pt–Ru efficiency in ethanol oxidation were declared in [473]. However, the efficiency was confirmed in [474]. Hable and Wrighton [475] demonstrated that Pt–Ru in polyaniline matrix is a more active catalyst for ethanol oxidation than Pt in the same configuration.

Wang et al. [476] started with a problem of direct ethanol fuel cell as a practical goal. They found a possibility to attain fuel cell characteristics very close to that already achieved for DMFC, despite their predominating product in phosphoric acid electrolyte being ethanal. These authors tested also 1- and 2-propanol, which formed propanal and acetone, respectively.

Ethanol oxidation on Au-supported electrodeposited Pt–Ru [477], in contrast to [476], resulted in preferential CO_2 formation. CO_2 and acetaldehyde were found by means of DEMS technique when ethanol was oxidized on Pt–Ru at 5–40 °C. Optimal alloy composition was reported to be temperature-dependent 33 at.% Ru for 5 and 15 at.% Ru for 40 °C.

The comparative study of various low molecular alcohols oxidation [478] involved ethanol, ethylene glycol, *n*-propanol, and *n*-buthanol. Ethanol oxidation on Pt–Ru was concluded to be of practical interest.

At low anodic potentials, the activity of Pt–Ru towards ethanol oxidation exceeds not only the activity of Pt but of Pt–Mo alloy as well, as it follows from voltammetry, chronopotentiometry, and DEMS data [479].

Recently, Iwasita's group completed a number of studies of ethanol and acetaldehyde oxidation [480–484]. They found rather narrow region of catalyst composition providing Pt–Ru activity in this reaction (about 40 at.% Ru), while for methanol oxidation, much wider region 10–45 at.% corresponded to high activity. Probably, just the necessity to use a narrow interval of Pt/Ru ratios induces some disagreements in conclusions of various authors concerning ethanol oxidation on Pt–Ru.

FTIR was applied to identify ethanol oxidation products (CO_2, acetaldehyde, and acetic acid). The increase of Ru content was found to enhance the formation of acetic acid. The proposed reaction scheme looks as follows:

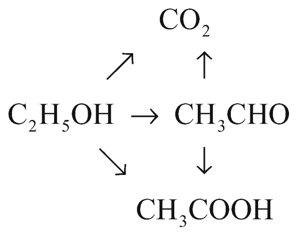

$$\begin{tikzcd} & CO_2 \\ C_2H_5OH \arrow[ur] \arrow[r] \arrow[dr] & CH_3CHO \arrow[u] \arrow[d] \\ & CH_3COOH \end{tikzcd}$$

Langmuir–Hinshelwood mechanism was assumed for ethanol oxidation.

Leger et al. [485] also applied FTIR to study this reaction and proposed another scheme with slightly different pathways. We should stress that the interest to ethanol oxidation increased essentially during the recent years.

Tarasevich et al. [486] started with ethanol oxidation on Ru–Ni in basic media and declared some practical prospects of this catalyst. A number of this and other studies [201, 221, 487–491] were aimed to the search for optimized Pt–Ru catalyst, its modification, and understanding of ethanol electrooxidation mechanism.

Ethylene glycol oxidation is also considered as being of interest for applications. A study of Peled et al. [492] confirmed that ethylene glycol fuel cell is competitive with DMFC, especially for practical electric vehicles. FTIR study [493] discovered the presence of oxalic and glycolic acid in the mixture of ethylene glycol oxidation products when Pt–Ru catalyst was used in acidic medium. Recently, Wang et al. [494, 495] started a systematic DEMS study of this reaction on various materials including Pt–Ru to characterize the products and to estimate the efficiency of various reaction steps.

Ethylene glycol oxidation on Pt–Ru in basic medium [496] demonstrated lower activity of this catalyst as compared to other materials studied for comparison.

Other fuels listed in the beginning of this section tend to hydrolysis at elevated temperatures with formation of a mixture containing methanol and formic acid. This decomposition takes place in the absence of catalyst. The following scheme of trimethoxymethane oxidation based on online mass spectroscopy and FTIR data [497] was proposed:

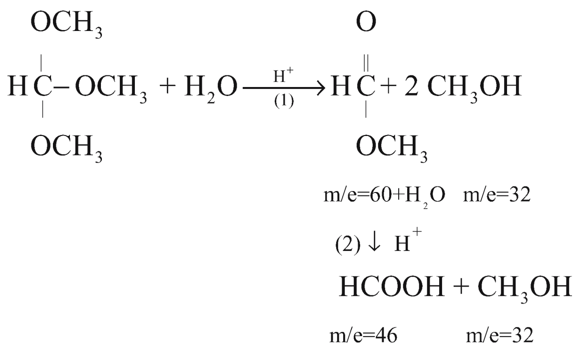

$$\underset{\substack{|\\ OCH_3}}{\overset{\substack{OCH_3\\ |}}{HC}}\!-\!OCH_3 + H_2O \xrightarrow[(1)]{H^+} \underset{\substack{|\\ OCH_3}}{\overset{\substack{O\\ \|}}{HC}} + 2\,CH_3OH$$

$$\text{m/e=60+}H_2O \quad \text{m/e=32}$$

$$(2)\downarrow H^+$$

$$\underset{\text{m/e=46}}{HCOOH} + \underset{\text{m/e=32}}{CH_3OH}$$

As the formic acid is oxidized much faster than methanol, its formation should be considered as a key factor for the improvement of the anode performance by using trimethoxymethane instead of methanol. This conclusion is valid at elevated temperatures exclusively, as the hydrolysis is too slow at ambient temperature. Findings of Savilell et al. related to electrooxidation of fuels tending to hydrolysis stimulate the studies of fuel mixtures.

The efficiency of Pt–Ru as a catalyst for formic acid oxidation was reported [308], and the highest activity was found for Pt/Ru=1:1 ratio, like for CO oxidation.

Oxidation of glycerol should be also mentioned, being of interest for fuel cells with simultaneous electrosynthetic function [498]. For glycerol, high oxidation rate was found in experiments with Ru-doped Pd–Pt catalysts in polyaniline matrix. Savadogo and Yang [499] compared the rates of ethylal, dioxolane, and methanol oxidation on Pt, Pt–RuO_2, Pt–Ru, and other materials. They concluded possible competitiveness of some acetals and methanol. The addition of RuO_2 decreased ethylal oxidation overvoltage for >200 mV. It was assumed that this reaction follows via hydronium ion catalyzed hydrolysis step

$$(CH_3O)_2(CH_2)_3 + 3H_2O \overset{H^+}{\rightleftharpoons} 4CH_3OH + CH_2O$$

with the subsequent oxidation of methanol and formaldehyde formed in the course of hydrolysis

$$CH_2O + 4CH_3OH + 5H_2O \rightleftharpoons 5\,CO_2 + 28H^+ + 28e$$

(the total number of transferred electrons is 28).

Pt–Ru was concluded to be the most active alloy for dimethyl ether oxidation at 50 °C and potentials below 0.5 V (RHE) [500].

Ru-containing anode materials were also tested in direct oxidation of hydrocarbons at 600 °C in solid electrolyte cell [501]. Oxidation of ammonia [502] and CO_2 reduction to formic acid with 90% yield [503] on Pt–Ru were also reported.

Conclusions

We attempted to demonstrate the pronounced progress in design and characterization of highly efficient platinum–ruthenium electrocatalysts and the evident possibility to work out DMFC using this type of catalysts. There are also no doubts that the current level of basic electrocatalytic studies is already close to fundamental level of modern heterogeneous catalysis. By adding the comparative analysis of experimental techniques (it can be found for example in review [32]), one can get a representative view of electrocatalysis state-of-the art in general. Pt–Ru system appears to be much more complex than single-element catalysts. At the same time, its choice for so detailed studies is justified by its prominent characteristics required by applications. The experience of these studies is expected to be actual for future understanding of even more complex catalysts. It is also evident that we still meet a number of intriguing problems requiring further efforts to be solved.

One of these problems is related to understanding of the role of Pt–Ru elemental composition. All hypotheses one can find in the literature (including traditional geometric models and simplified considerations of electronic effects) are unable to explain the available set of experimental data, and final conclusion remains a matter of future. The same is concerned to the role of support and size effects.

Structural sensitivity of CO and organic fuels electrooxidation is well documented by single-crystal experiments, as well as by the observed dependences on the shape and size of isolated nanoparticles. New model systems imitating the features of real catalysts are necessary to understand the role of various edge regions, including defective intergrain regions. How should one make a choice of a model system? Homogeneous distribution of particles can be provided by lithography, but this technique gives no chance to obtain particle size below 50 nm. More dispersed materials result from chemical deposition, but stabilization of particles always requires some surfactant, which, in its turn, affects catalytic activity.

A general danger of using less homogeneous materials consists in averaging of the properties of a large set of nanoparticles having different individual properties. In relation to this problem, the recent studies of single nanoparticles in STM configuration look promising but rather complicated for understanding of size effects. Systems being surely of interest are ultrathin layers of foreign metals on single-crystalline surfaces and the experiments with these systems can give the unique information if the role of interactions clarified.

It is surely an actual problem to find DMFC catalysts more effective than Pt–Ru among ternary and more complex systems. Already considered candidates are Pt–Ru–Mo, Pt–Ru–W_2C, Pt–RuWO_x, Pt–Ru–Sn, Pt–Ru–Ni. They give a chance to obtain cheaper catalysts without decrease of activity and stability. A brief review on ternary and four-component catalysts can be found in [504] (see also the recent papers [505–507]. We believe that the winners with extremely high catalytic activity can be found among ternary systems, like Pt–Ru remains a well-known winner among binary systems. However, any final conclusions can be done only after numerous experiments and tests, like already known for Pt–Ru. Combinatorial approaches can be applied to intensify optimization and search.

From a theoretical point of view, the problems of adsorbate dynamics and surface diffusion remain extremely important, as well as general molecular modeling of electrocatalytic reaction layers. The latter problem requires a solid knowledge of the nature of adsorbed species taking part in the limiting reaction step. Numerous experimental efforts, especially in the field of IR spectroscopy, still gave no exact understanding of this problem. Some optimistic expectations are related to optical techniques of visible region, especially second harmonic generation.

Among still unsolved problems, one should mention methanol dehydrogenation mechanism (subsequent or concerted, it is easier to rupture hydrogen bonded with carbon or with oxygen atom). Some data demonstrate the difference of CO species resulting from CO and methanol adsorption, and the reasons are not yet understood. It should be noted that direct adsorption measurements are usually carried out at room temperature, while the real catalysts operate at elevated temperatures.

Deeper penetration into electrocatalysis mechanisms is of crucial importance. If to discuss CO electrooxidation as an example, one should consider at least two general types of CO oxidation mechanisms [80]. For Pt–Ru (and Pt–Re), the systems with CO adsorption taking place on any site, the pseudo-bifunctional mechanism operates:

$$\mathrm{Pt-Ru-CO_{ad}+Ru-OH_{ad}\rightarrow CO_2+H^++e}$$

This is supported by the increase of CO oxidation overvoltage with CO pressure (negative reaction order in relation to CO) because of competitive CO and OH adsorption. For Pt–Sn and Pt–Mo, bifunctional mechanism works in its classical version, as CO is never adsorbed on Sn and Mo atoms bonding OH species exclusively:

$$\mathrm{Pt-CO_{ad}+Sn(Mo)-OH_{ad}\rightarrow CO_2+H^++e}$$

Positive reaction order in relation to CO was found for Pt_3Sn. This means that the traditional classification of adatoms (oxophylic and not adsorbing oxygen) should be reconsidered, as well as the models of synergetic effect.

For methanol oxidation at low temperatures, when methanol is adsorbed on platinum exclusively, we can continue to deal with a classical version of bifunctional mechanism. However, when the temperature increases, we must extend our consideration to pseudo bifunctionality.

Currently, available level of theory and computational techniques does not allow any quantitative predictions, but already gives a chance to understand deeper the role of electronic structure of catalyst in electrocatalysis despite numerous complications (even more pronounced than in gas phase catalysis). A number of groups started with modeling electrocatalytic systems [508–523]. Ab initio calculations demonstrated that the presence of Ru decreases adsorbate bonding with Pt atoms. Ab initio comparative analysis of CO oxidation on Pt and Pt_2Ru was reported by Neurock et al., and some new tendencies were found, being of importance to clarify bifunctional mechanism. Ab initio molecular dynamics simulations of OH adsorption on Pt–Ru alloy in presence of water demonstrated that OH species formed on Ru can easily induce H–O bond rupture in water molecule adsorbed at the neighboring Pt atom. This rather essential mechanism corresponding to effective transfer of adsorbed OH from Ru to Pt was recently confirmed in [519]. Taking into account this result, as well as the results of CO adsorption modeling on bimetallic surfaces [518], one should reconsider the bifunctional mechanism. Quantum chemistry and general computational approaches are expected to play the increasing role in the studies of electrocatalytic systems, especially for catalysts consisting of nanoclusters.

Deeper penetration into Pt–Ru electrocatalysis mechanism will open new problems contributing to further improvement of fuel cells.

Acknowledgements I am grateful to Prof. G.A. Tsirlina for her active stimulating criticism in the course of review preparation. I would like to acknowledge the referees whose valuable remarks were extremely helpful. Pt–Ru research is supported by RFBR, project 05-03-32592a.

References

1. Petrii OA (2004) Chem Ind 58:280
2. Wohler F (1868) Ann Chem Pharm (Lieb) 146:375
3. Holborn L, Day A (1900) Ann Phys 2:505
4. Nemilov VA, Rudnitzkii AA (1937) Izv AN SSSR OMEN 1:3
5. Ageev NV, Kuznetzov VG (1937) Izv AN SSSR OMEN 1:753
6. Amano A, Parravano G (1957) Adv Catal 9:733
7. Gray TJ, Masse NG, Oswin HG (1960) Congr Intern Catalyse, Paris 2:977 2(1960)977
8. McKee DW, Norton FJ (1964) J Phys Chem 8:481
9. McKee DW (1965) Trans Far Soc 61:2273
10. Petrii OA (1965) Dokl AN SSSR 160:871
11. Petrii OA, Kazarinov VE (1965) Elektrokhimija 1:1389
12. Petrii OA, Podlovchenko BI, Frumkin AN, Hira L (1965) J Electroanal Chem 11:12
13. Petrii OA, Entina VS, Shelepin IV (1966) Elektrokhimija 2:457
14. Marvet RV, Petrii OA (1967) Elektrokhimija 3:116
15. Entina VS, Petrii OA, Zhitnev Y (1967) Elektrokhimija 3:344
16. Entina VS, Petrii OA, Risikova VT (1967) Elektrokhimija 3:758
17. Entina VS, Petrii OA (1967) Elektrokhimija 3:1237
18. Entina VS, Petrii OA (1968) Elektrokhimija 4:110
19. Entina VS, Petrii OA (1968) Elektrokhimija 4:457
20. Entina VS, Petrii OA (1968) Elektrokhimija 4:678
21. Bockris JOM, Wroblowa H (1964) J Electroanal Chem 7:428
22. Adlhart OJ, Hever KO. Fuel cell catalysis. Final report; Contract DA36-039,SC-90691, US Army Electronics Research and Development Laboratories. Report 4, 1/10/63-31/3/64
23. Cohn JGE, Adlhart OJ (1963) Fuel cells. Belg. Pat. 650,651, Jan. 18 (1965); US Appl. July 17
24. Adlhart OJ (1965) Proc Ann Power Sources Conf 19:1
25. Adlhart OJ, Shields H, Pudick S (1965) Engelhard Ind Tech Bull 6:37
26. Adlhart OJ, Hartner AJ (1966) Engelhard Ind Tech Bull 6:104
27. Binder H, Kohling A, Sandstede G (1965) In: Baker S (ed) Hydrocarbon fuel cell technol. Academic, New York, p 91
28. Binder H, Kohling A, Sandstede G (1972) In: Sandstede G (ed) Electrocatalysis to fuel cells. University of Washington Press for Batelle Research Center, Seattle, p 43
29. Petrii OA (1969) Progress elektrokhimii organicheskih soedinenii. T.1. M.: Nauka, S.278–326
30. Parsons R, VanderNoot TJ (1988) J Electroanal Chem 257:9
31. Hamnett A (1997) Catal Today 38:445
32. Wasmus S, Kuver A (1999) J Electroanal Chem 461:14
33. Vielstich W, Lamm A, Gasteiger HJ (eds) Handbook of fuel cell technology (2003). Wiley, New York
34. Vogel W, Britz P, Bonnemann H, Rothe J, Hormes J (1997) J Phys Chem B 101:11029
35. Gavrilov AN, Petrii OA, Mukovnin AA, Smirnova NV, Levchenko TV, Tsirlina GA (2007) Electrochim Acta 52:2775
36. Frumkin AN, Podlovchenko BI (1963) Dokl AN SSSR 150:349
37. Kim JY, Yang ZG, Chang C-C, Valdez YI, Narayanan SR, Kumta PN (2003) J Electrochem Soc 159:A1421
38. Niedrach LW, McKee DW, Paynter J, Danzig IF (1967) Electrochem Technol 5:318
39. McKee D, Scarpellino A (1968) Electrochem Technol 6:101; Pat.Fr. 1,560,969 (Cl.Ho1m), 21 mar.1968; US Appl. 26 Apr. 1967 (Chem. Abstr. 1970.72:38291V)
40. Sokol’skii DV, Novikova ZN (1972) Adsorbtzia i dvoinoi elektricheskii sloi v elektrokhimii,M., Nauka 112–118
41. Batzold JS, Geyer J, Beltzer M, Pat BRD Offen 2, 263, 636 (Cl H01m), 12 jul. 1973, US Appl 213, 556, 29 Dec 1971
42. Sokol’skii DV, Djardamalieva KК, Dukhovnaia TM (1969) Zh phis khim 43:505
43. Hoar TP, Brooman CW (1966) Electrochim Acta 11:545 (1966) Platinum Met Rev 10:135
44. Appleby AJ (1970) J Electrochem Soc 117:1159
45. Adlhart OJ (1968) Frontiers in fuel cells 7:2
46. Fasman AB, Isabekov A, Akmashev BК (1968) Zh phis khim 42:903
47. Watanabe M, Takashi S, Motoo S (1972) Denki kagaku 40:210
48. Kim TI, Grishina TM, Vovchenко GD (1972) Zh phis khim 46:960
49. Yanкovskii XI, Semenova AD, Vovchenко GD (1973) Vestnik MGU ser khim 14:83
50. Brintzeva VI, Dunaev Y (1975) Кinetika i mekhanism elektrodnih reaktzii, Izd AN Кazakhskoi SSR, Alma-Ata, 53–62
51. El Quebly MA, Haissinsky M (1954) J Chim Phys 51:290
52. Zviagintzev OE, Кolbin NI, Riabov AN, Avtокratova DA, Gorunov AA (1965) Analiticheskaja khimia elementov. Rutenii. M. Nauka
53. Kobayashi Y, Yamatera H, Okumo H (1965) Bull Chem Soc Jpn 38:1911
54. Buckley RR, Mercer EE (1966) J Phys Chem 70:3103
55. Harrison JA, Philippart (1972) J Electroanal Chem 40:357

56. Eichner P (1967) Bull Soc Chim France 2051
57. Fleischmann M, Koryta J, Thirsk HR (1967) Trans Far Soc 63:1261
58. Kuhn AT, Wright PM (1970) J Electroanal Chem 27:319
59. Giles RD, Harrison JA, Thirsk HR (1969) J Electroanal Chem 20:47
60. Fleischmann M, Grenness M (1972) J Chem Soc Faraday Trans I 68:2305
61. Cotton TM, Woolf AA (1962) Anal Chem 34:375
62. Gorunov AA, Ryabov AN (1965) Zh Neorg Khim 10:2596
63. Llopis J, Tordesillas IM, Alfayate JM (1966) Electrochim Acta 11:623, 633
64. Llopis J, Gamboa JM, Alfayate JM (1967) Electrochim Acta 12:57
65. Stoyanovskaya TN, Khomchenko GP, Vovchenko GD (1962) Vestnik MGU Ser Khim 5:30 (1963) ibid 2:20; (1965) ibid 2:56; 3:64; 4:51
66. Stoyanovskaya TN, Khomchenko GP, Vovchenko GD (1964) Zh phis khim 38:434
67. Mashкova LP, Pletushkina AI (1965) Vestnik MGU Ser Khim 5:52
68. Taran RB, Khomchenko GP (1968) Vestnik MGU Ser Khim 6:83
69. Mashкova LP, Pletushkina AI, Khomchenko GP (1968) Vestnik MGU Ser Khim 6:104
70. Pletushkina AI, Mashкova LP, Krilova NN (1970) Vestnik MGU Ser Khim 3:317
71. Mashкova LP, Pletushkina AI, Khomchenko GP (1969) Vestnik MGU Ser Khim 1:83
72. Grishina TM, Vovchenko GD (1972) Zh phis khim 46:960
73. Podviazkin YA, Grechushkina GP (1970) Zh phis khim 44:2529
74. Watanabe M, Suzuki T, Motoo S (1970) Denki Kagaku 38:927
75. Watanabe M, Suzuki T, Motoo S (1971) Denki Kagaku 39:394
76. Watanabe M, Suzuki T, Motoo S (1972) Denki Kagaku 40:205, 210
77. Watanabe M, Motoo S (1973) Denki Kagaku (presently Electrochemistry) 41:190
78. Watanabe M, Motoo S (1975) J Electroanal Chem 60:267, 275
79. Janssen MMP, Moolhuysen J (1976) Electrochim Acta 21:861, 869
80. Markovic NM, Ross PN Jr (2002) Surf Sci Reports 45:117
81. Adzic R (2003) Encyclopedia of electrochemistry, vol 1. Gileadi E and Urbakh M (eds) Wiley, p 471, New York
82. Shropshire JA (1965) J Electrochem Soc 112:465; (1967) J Electrochem Soc 114:773
83. Watanabe M, Uchida M, Motoo S (1987) J Electroanal Chem 229:395
84. Hamnett A, Kennedy BJ (1988) Electrochim Acta 33:1613
85. Goodenough JB, Hamnett A, Kennedy BJ, Manoharan R, Weeks SA (1988) J Electroanal Chem 240:133; (1990) Electrochim Acta 35:199
86. Swathirajan S, Mikhail YM (1991) J Electrochem Soc 138:1321
87. Hutchinson JM (1972) Plat Met Rev 16:88
88. Filatov DK, Poljakova VP, Roshan NR, Savitzkii EM, Skundin AM (1978) Elektrokhimija 14:132
89. Beden B, Kadirgan F, Lamy C, Leger JM (1981) J Electroanal Chem 127:75
90. McNicol BD (1981) J Electroanal Chem 118:71
91. Venkateswara RK, Roy CB (1982) Indian J Chem 21A:34
92. Aramata A (1980) J Phys Chem 84:376
93. Ramesh KV, Sarode PR, Vasudevan S, Shukla AK (1987) J Electroanal Chem 223:91
94. Fedotova TG, Martiniuk GA, Khomchenko GP (1973) Zh phis khim 47:112
95. McNicol BD, Short RT (1977) J Electroanal Chem 81:249
96. Alerasool S, Boecker D, Rejai B, Gonzalez RD, Del Angel G, Azomosa M, Gomez R (1988) Langmuir 4:1083
97. Ross PN, Kinoshita K, Scarpellino AJ, Stonehart P (1975) J Electroanal Chem 63:97
98. Hughes VB, Miles R (1983) J Electroanal Chem 145:87
99. Aramata A, Kodera T, Masuda M (1988) J Appl Electrochem 18:577
100. Aramata A, Masuda M (1991) J Electrochem Soc 138:1949
101. Meli G, Leger J-M, Lamy C, Durand R (1993) J Appl Electrochem 23:197
102. Kawashima A, Hashimoto K (1981) Proceedings of the 4th International Conference on Rapidly Quenched Metals (Sendai) p 1427; Hara M, Hashimoto K, Masumoto T Ibid, p 1423
103. Aramata A (1989) Ext Abstr 40th ISE Meeting, Kyoto, p 1252
104. Hilaire L, Diaz Guerrero G, Legare P, Maire G, Krill G (1984) Surf Sci 146:569
105. Wolf GK, Zucholl K, Folger H, O'Grady (1983) Nucl Instrum Methods 209–210:835
106. Szabo S, Bakos I (1987) J Electroanal Chem 230:233
107. McNicol BD, Short RT (1978) J Electroanal Chem 92:115
108. Quiroz MA, Gonzalez I, Meas Y, Lamy-Pitara E, Barbier J (1987) Electrochim Acta 32:289
109. Arikado T, Iwakura C, Tamura H (1977) Electrochim Acta 22:229
110. Al'-Ata GA, Krasnova NN, Poljakova VP, Zuikova VS, Grjaznov VM, Vassiliev Y, Savitzkii EM (1974) Elektrokhimija 10:855
111. Krasnova NN, Khomchenko GP, Poljakova VP, Vassiliev Y (1975) Elektrokhimija 11:495
112. Ticianelli E, Beery JG, Paffett MT, Gottesfeld S (1989) J Electroanal Chem 258:61
113. Penckert M, Coenen FP, Bonzel HP (1984) Electrochim Acta 29:1305
114. Caram JA, Gutierrez C (1990) J Electroanal Chem 291:289
115. Zavadil KR, Ingersoll D, Rogers JW Jr (1991) J Electroanal Chem 318:223
116. Cao EY, Stern DA, Gui JY, Hubbard AT (1993) J Electroanal Chem 354:71
117. Barral G, Diard J-P, Montella C (1986) Electrochim Acta 31:277
118. Nikol'skii AB (1963) J inorg khim 8:541, 668
119. Doblhofer K, Metikos M, Ogumi Z, Gerischer H (1981) Ber Bunsenges Phys Chem 122:395
120. Trasatti S, O'Grady WE (1981) Adv Electrochem Electrochem Eng 12:177
121. Hadzi-Jordanov S, Angerstein-Kozlowska H, Conway BE (1975) J Electroanal Chem 60:359
122. Hadzi-Jordanov S, Angerstein-Kozlowska H, Vukovic M, Conway BE (1977) J Phys Chem 81:2271
123. Hadzi-Jordanov S, Angerstein-Kozlowska H, Vukovic M, Conway BE (1978) J Electrochem Soc 125:1471
124. Birss V, Myers R, Angerstein-Kozlowska H, Conway BE (1984) J Electrochem Soc 131:1502
125. Mitchell D, Rand DAJ, Woods R (1978) J Electroanal Chem 89:11
126. Buckley DN, Burke LD (1975) J Chem Soc Faraday Trans I 71:1447 (1976) ibid 72:2431
127. Burke LD, Mulcahy JK, Venkatesan S (1977) J Electroanal Chem 81:339
128. Kinoshita K, Ross PN (1977) J Electroanal Chem 78:313
129. Deriagina OG, Tomashov ND (1981) Elektrokhimija 17:1238
130. Pecherskii MM, Gorodetskii VV, Pulina VM, Losev VV (1976) Elektrokhimiya 12:1445
131. Lezna RO, De Tacconi NR, Arvia A (1983) J Electroanal Chem 151:193
132. Vedenjapin AA, Zubareva ND, Klabunovskii EI, Godiascheva IP, Rubtzov IA (1975) Zh Phiz Khimii 49:1480
133. Zakumbaeva GD, Beketaeva LA, Shapovalova LB (1978) React Kinet Catal Lett 8:235

134. Breiter MW (1984) J Electroanal Chem 178:53 (1986) J Electroanal Chem 214:547
135. Bagotzky VS, Skundin AM, Tuseeva EK (1976) Electrochim Acta 21:29
136. Kost KM, Bartak DE, Kazee B, Kuwana T (1990) Anal Chem 62:151
137. Quiroz MA, Meas Y, Lamy-Pitara E, Barbier J (1983) J Electroanal Chem 157:165
138. Quiroz MA, Gonzalez I, Vargas H, Meas Y, Lamy-Pitara E, Barbier J (1986) Electrochim Acta 31:277
139. Christmann K, Ertl G, Shimizu H (1980) J Catal 61:397
140. Nguyen van Huong C, Gonzalez-Tejera MJ (1988) J Electroanal Chem 244:249
141. Adzic RR, Anastasijevic NA, Dimitrijevic ZM (1984) J Electrochem Soc 131:2730
142. Quiroz MA, Saldago L, Meas Y (1988) Electrochim Acta 33:435
143. Quiroz MA, Saldago L, Gonzalez I, Meas Y, Rojas-Hernandez A (1989) J Electroanal Chem 261:409
144. Trasatti S (1983) Electrochim Acta 28:1083
145. Horanyi G, Rizmayer EM (1984) J Electroanal Chem 181:199
146. Horanyi G, Veres A (1986) J Electroanal Chem 205:259
147. Miles MH, Klaus EA, Gunn BP (1978) Electrochim Acta 23:521
148. Kotz R, Lewerenz HJ, Bruesch P, Stucki S (1983) J Electroanal Chem 150:209
149. Kotz R, Lewerenz HJ, Stucki S (1983) J Electrochem Soc 130:825
150. Wohlfahrt-Mehrens M, Heitbaum J (1987) J Electroanal Chem 50:251
151. Anderson DP, Warren LF (1984) J Electrochem Soc 131:347
152. Miles A, Davies HL (1992) Electrochim Acta 37:1217
153. Gallizioli G, Tandardini F, Trasatti S (1975) J Appl Electrochem 5:203
154. Kotz ER, Stucki S (1987) J Appl Electrochem 17:1190
155. Bindra P, Gerischer H, Kolb DM (1977) J Electrochem Soc 124:1012
156. Weininger JL, Russell RR (1978) J Electrochem Soc 125:1482
157. Tomkiewicz M, Huang YS, Pollak FH (1983) J Electr Sci Technol 7:1514
158. O’Grady WE, Goel AK, Pollak FH, Park HL, Huang YS (1983) J Electroanal Chem 151:295 (O’Grady WE, Atanasoska Lj, Pollak FL, Park HL (1984) J Electroanal Chem 178:1984)
159. Ardizzone S, Siviglia P, Trasatti S (1981) J Electroanal Chem 122:395
160. Fokkink LGJ, de Keizer A, Kleijn JM, Lyklema J (1986) J Electroanal Chem 208:401
161. Kuo K-N, Moses PR, Lenhard JR, Green DC, Murray RW (1979) Anal Chem 51:745
162. Saddon EA, Saddon KR (1984) The chemistry of ruthenium. Elsevier, New York
163. Pletcher D (1984) J Appl Electrochem 14:403
164. Kelley SC, Degula GA, Smyrl WH (2000) Electrochem Solid State Lett 3:407
165. Motokawa S, Mohamedi M, Momma T, Osaka T, Shoji S (2004) Electrochem Commun 6:562
166. Sugimoto W, Yokoshima K, Ohuchi K, Murakami Y, Takasu Y (2006) J Electrochem Soc 153:A255
167. Radmilovich V, Gasteiger HA, Ross PN (1995) J Catal 154:98
168. Pan Ch, Dassenoy F, Casanove M-J, Philippot K, Amiens C, Lecante P, Mosset A, Chaudret B (1999) J Phys Chem B 103:10098
169. Steigerwalt ES, Degula GA, Cliffel DE, Lukehart CM (2001) J Phys Chem B 105:8097
170. Jiang L, Sun G, Zhao X, Zhou Z, Yan S, Tang S, Wang G, Zhou B, Xin Q (2005) Electrochim Acta 50:2371
171. Okada T, Arimura N, Ono C, Yuasa M (2005) Electrochim Acta 51:1130
172. Orth SD, Terry MR, Abboud K, Dodson B, McElwee-White L (1996) Inorg Chem 35:916
173. Sterenberg BT, Jennings MC, Puddephatt RJ (1999) Organometallics 18:2162
174. Gotz M, Wendt H (1998) Electrochim Acta 43:3637
175. Rao V, Simonov PA, Savinova ER, Plaksin GV, Cherepanova SV, Kryukova GN, Stimming U (2005) J Power Sources 145:178
176. Savinova ER (2006) DSc thesis, Boreskov Inst, Novosibirsk
177. Antolini E, Cardellini F (2001) J Alloys Comp 315:118
178. Lim CH, Scott K, Allen RG, Roy S (2004) J Appl Electrochem 34:929
179. Wang X, Hsing I-M (2003) J Electroanal Chem 556:117
180. Tsai M-C, Yeh T-K, Trai C-H (2006) Electrochem Commun 8 (9):1445
181. Wang H, Jusys Z, Behm RJ (2006) J Appl Electrochem 36:1187
182. Tsai M-C, Yeh T-K, Chen C-Y, Tsai C-H (2007) Electrochem Commun 9:2299
183. Prabhuram J, Zhao TS, Liang ZX, Chen R (2007) Electrochim Acta 52:2649
184. Selvaraj V, Alagar M (2007) Electrochem Commun 9:1145
185. Dojkovic SL, Vidakovic TR, Durovic DR (2003) Electrochim Acta 48:3607
186. Giorgi L, Antolini E, Pozio A, Passalacqua E (1998) Electrochim Acta 43:3675
187. Mukerjee S, Lee SJ, Ticianelli EA, McBreen J, Grgur BN, Markovich NM, Ross PN, Giallombardo JR, De Castro ES (1999) Electrochem Solid-State Lett 2:12
188. Schmidt TJ, Gasteiger HA, Behm RJ (1999) Electrochem Comm 1:1
189. Bonnemann H, Brinkmann R, Britz P, Endruschat U, Mortel R, Paulus UA, Feldmeyer GJ, Schmidt TJ, Gasteiger HA, Behm RJ (2000) J New Mater Electrochem Syst 3:199
190. Luna AMC, Camara GA, Paganin VA, Ticianelli EA, Gonzalez ER (2000) Electrochem Commun 2:222
191. Silva RF, De Francesco M, Giorgi L, Campa MC, Cardellini F, Pozio A (2004) J Solid-State Electrochem 8:544
192. Okada T, Ayato Y, Yuasa M, Sekine I (1999) J Phys Chem B 103:3315
193. Okada T, Ayato Y, Satou H, Yuasa M, Sekine I (2001) J Phys Chem B 105:6980
194. Su Y, Xue X, Xu W, Liu C, Xing W, Zhou X, Tian T, Lu T (2006) Electrochim Acta 51(20):4316
195. Han KI, Lee JS, Park SO, Lee SW, Park YW, Kim H (2004) Electrochim Acta 50:791
196. Frackowiak E, Lota G, Cacciaguerra T, Beguin F (2006) Electrochem Comm 8:129
197. Liu Y-C, Qiu X-P, Huang Y-Q, Zhu W-T, Wu G-S (2002) J Appl Electrochem 32:1279
198. Roth C, Martz N, Hahn F, Leger J-M, Lamy C, Fuess H (2002) J Electrochem Soc 149:E433
199. Yang LX, Allen RG, Scott K, Christensen PA, Roy S (2005) Electrochim Acta 50:1217
200. Shao Z-G, Lin W-F, Zhu F, Christensen PA, Li M, Zhang H (2006) Electrochem Commun 8:5
201. Chetty R, Scott K (2007) Electrochim Acta 52:4073
202. Macak JM, Barczuk PJ, Tsuchiya H, Nowakowska MZ, Ghicov A, Chojak M, Bauer S, Virtanen S, Kulesza PJ, Schmuki P (2005) Electrochem Commun 7:1417
203. Hepel M, Kumarihamy I, Zhong CJ (2006) Electrochem Commun 8(9):1439
204. Hepel M, Dela I, Hepel T, Luo J, Zhong CJ (2007) Electrochim Acta 52:5529
205. Tian J, Sun G, Jiang L, Yan Sh, Mao Q, Xin Q (2007) Electrochem Commun 9:563
206. Wang J, Muzameh M, Laocharoensuk R, Gonzales-Garcia O, Gervasio D (2000) J Electrochem Commun 8:1106

207. Chen R, Zhao TS (2007) Electrochem Commun 9:718
208. Chen L, Guo M, Zhang H-F, Wang X-D (2006) Electrochim Acta 52:1191
209. Barczuk PJ, Miecznikowski K, Kulesza PJ (2007) J Electroanal Chem 600:80
210. Lu GQ, Wang CY, Yen TJ, Zhang X (2004) Electrochim Acta 49:821
211. Saha MS, Li R, Su X (2007) Electrochem Commun 9:2229
212. Bock C, Collier A, MacDougall B (2005) J Electrochem Soc 152 (12):A2291
213. Denis MC, Gouerec P, Guay D, Dodelet JP, Lalande G, Schulz R (2000) J Appl Electrochem 30:1243
214. Angelucci CA, D’Villa S, Nart FC (2007) Electrochim Acta 52:7293
215. Lizcano-Valbuena WH, Paganin VA, Gonzalez ER (2002) Electrochim Acta 47:3715
216. Zhou Z, Wang S, Zhou W, Wang G, Jiang L, Li W, Song S, Liu J, Sun G, Xin Q (2003) Chem Commun 394
217. Yan S, Sun G, Tian J, Jiang L, Qi J, Xin Q (2006) Electrochim Acta 52:1692
218. Colmenares L, Wang H, Jusys Z, Jiang L, Yan S, Sun GQ, Behm RJ (2006) Electrochim Acta 52:221
219. Yan S, Sun G, Tian J, Jiang L, Qi J, Xin Q (2006) Electrochim Acta 52:1692
220. Liu Z, Hong L (2007) J Appl Electrochem 37:505
221. Li H, Sun G, Cao L, Jiang L, Liu Q (2007) Electrochim Acta 52:6622
222. Lee S-A, Park K-W, Choi J-H, Kwon B-K, Sung Y-E (2002) J Electrochem Soc 149:A1299
223. Pozio A, Silva RF, Francesco MD, Cardellini F, Giorgi L (2003) Electrochim Acta 48:1627
224. Xue X, Ge J, Liu Ch, Xing W, Lu T (2006) Electrochem Commn 8:1280
225. Rahue BR, McLarnon FR, Cairns EJ (1995) J Electrochem Soc 142:1073
226. McBreen J, Mukerjee S (1995) J Electrochem Soc 142:3399
227. He C, Kunz HR, Fenton JM (1997) J Electrochem Soc 144:970
228. Li X, Hsing I-M (2006) Electrochim Acta 52:1358
229. Bock C, Paquet C, Couillard M, Botton GA, MacDougall BR (2004) J Am Chem Soc 126:8028
230. Liu L, Pu C, Viswanathan R, Fan Q, Liu R, Smotkin ES (1998) Electrochim Acta 43:3657
231. Arico AS, Antonucci PL, Modica E, Baglio V, Kim H, Antonucci V (2002) Electrochim Acta 47:3723
232. Dickinson AJ, Carrette LPL, Collins JA, Friedrich KA, Stimming U (2002) Electrochim Acta 47:3733
233. Jusys Z, Kaizer J, Behm RJ (2002) Electrochim Acta 47:3693
234. Suffredini HB, Tricoli V, Avaca LA, Vatistas N (2004) Electrochem Comm 6:1025
235. Bonnemann H, Brinkmann R, Brijoux W, Dinjus E, Joussen T, Korall B (1991) Angew Chem 103:1344
236. Schmidt TJ, Noeske M, Gasteiger HA, Behm RJ, Britz P, Brijoux W, Bonnemann (1997) Langmuir 14:2591
237. Vogel W, Britz P, Bonnemann H, Rothe J, Hormes J (1997) J Phys Chem B 101:11029
238. Schmidt TJ, Noeske M, Gasteiger HA, Behm RJ, Britz P, Bonneman H (1998) J Electrochem Soc 145:925
239. Nashner MS, Frenkel AI, Adler DL, Shapley JR, Nuzzo RG (1997) J Am Chem Soc 119:7760
240. Roth C, Martz N, Fuess H (2001) Phys Chem Chem Phys 3:315
241. Dubau L, Coutanceau C, Garnier E, Leger J-M, Lamy C (2003) J Appl Electrochem 33:419
242. Roth C, Goetz M, Fuess H (2001) J Appl Electrochem 31:793
243. Roth C, Papworth AJ, Hussain I, Nichols RJ, Schiffrin DJ (2005) J Electroanal Chem 581:79
244. Han K, Lee J, Kim H (2006) Electrochim Acta 52:1697
245. Li X, Hsing I-M (2006) Electrochim Acta 52:1358
246. Han K, Lee J, Kim H (2006) Electrochim Acta 52:1697
247. Vidakovic T, Christov M, Sundmacher K, Nagabhushana KS, Fei W, Kinge S, Bonnemann H (2007) Electrochim Acta 52:2277
248. Garcia G, Baglio V, Stassi A, Pastor E, Antonucci V, Arico AS (2007) J Solid-State Electrochem 11:1229
249. Goetz M, Wendt H (2001) J Appl Electrochem 31:811
250. Wang X, Hsing I-M (2002) Electrochim Acta 47:2981
251. Duteil A, Queau R, Chaudret B, Mazel R, Roucau Ch, Bradley JS (1993) Chem Mater 5:341
252. Solla-Gullon J, Vidal-Iglesias FG, Herrero E, Feliu JM, Aldaz A (2006) Electrochem Commun 8:189
253. Zhang X, Chan KY (2003) Chem Mater 15:451
254. Sine G, Duo I, El Roustom B, Foti G, Comninellis Ch (2006) J Appl Electrochem 36:847
255. Attard GS, Leclerc SAA, Maniguet S, Russel AE, Nandhakumar I, Bartlett PN (2000) Chem Mater 13:1444
256. Jiang J, Kucernak A (2003) J Electroanal Chem 543:187
257. Bauer A, Gyenge EL, Oloman CW (2006) Electrochim Acta 51:5356
258. Cheng TT, Gyenge EL (2006) Electrochim Acta 51:3904
259. Cheng TT, Gyenge EL (2006) Electrochim Acta 51:4497
260. Napporu WT, Leger J-M, Lamy C (1996) J Electroanal Chem 408:141
261. Kessler T, Castro-Luna AM (2002) J Appl Electrochem 32:825
262. Golali SM, Nozad A (2003) Electroanalysis 15:278
263. Choi J-H, Park K-W, Lee H-K, Kim Y-M, Lee J-S, Sung Y-E (2003) Electrochim Acta 48:2781
264. Camara GA, Giz MJ, Paganin VA, Ticianelli EA (2002) J Electroanal Chem 537:21
265. Sivakumar P, Ishak R, Tricoli V (2005) Electrochim Acta 50:3312
266. Sivakumar P, Tricoli V (2006) Electrochim Acta 51:1235
267. Xue X, Liu C, Xing W, Lu T (2006) J Electrochem Soc 153:E79
268. Chakraborty D, Bischoff H, Chorkendorff I, Johanessen T (2005) J Electrochem Soc 152(12):A2357
269. Xue X, Lu T, Liu Ch, Xu W, Su Y, Lu Y, Xing W (2005) Electrochim Acta 50:3470
270. He P, Liu H, Li Z, Li J (2005) J Electrochem Soc 152:E146
271. Su Y, Xue X, Xu W, Liu C, Xing W, Zhou X, Tian T, Lu T (2006) Electrochim Acta 51(20):4316
272. Urban PM, Funke A, Muller JT, Himmen M, Docter A (2001) Appl Catalysis A: General 221:459
273. Cattaneo C, Sanchez de Pinto MI, Mishima H, Lopez de Mishima HB, Lescano D, Cornaglia L (1999) J Electroanal Chem 461:32
274. Coutanceau C, Rakotondrainibe AF, Lima A, Garnier E, Pronier S, Leger J-M, Lamy C (2004) J Appl Electrochem 34:61
275. Lee CH, Lee CW, Kim DI, Jung DH, Kim CS, Shin DR (2000) J Power Sources 86:478
276. Metikos-Hukovic M, Omanovic S (1998) J Mol Catal A: Chemical 136:75
277. Park K-W, Sung Y-E, Toney MF (2006) Electrochem Commun 8:359
278. Morimoto Y, Yeager EB (1998) J Electroanal Chem 441:77
279. Natter H, Hempelmann R (2003) Electrochim Acta 49:51
280. Loffler M-S, Natter H, Hempelmann R, Wippermann K (2003) Electrochim Acta 48:3047
281. Rodriguez-Nieto FJ, Morante-Catacora TY, Cabrera CR (2004) J Electroanal Chem 571:15
282. Arico AS, Creti P, Antonucci PL, Cho J, Kim H, Antonucci V (1998) Electrochim Acta 43:3719
283. Tuseeva EK, Mikhailova AA, Khazova OA, Kurtakis KD (2004) Russ J Electrochem 40:1336

284. Tuseeva EK, Mikhailova AA, Khazova OA, Grinberg VA, Kurtakis KD (2005) Russ J Electrochem 41:1476
285. Havranek A, Wippermann K (2004) J Electroanal Chem 567:305
286. Page T, Johnson R, Hormes J, Noding S, Rambabu B (2000) J Electroanal Chem 485:34
287. Fujiwara N, Yasuda K, Ioroi T, Simora Z, Miyazaki Y (2002) Electrochim Acta 47:4079
288. Wei ZD, Chan SH (2004) J Electroanal Chem 569:23
289. Liu F, Wang C-Y (2005) Electrochim Acta 50:1413
290. Zhou X, Li S, Su Y, Lin C, Huang M, Lu T, Xing W (2006) J Electroanal Chem 588:129
291. Song JM, Miyatake K, Uchida H, Watanabe M (2006) Electrochim Acta 51(21):4497
292. Xu C, Shao TS, Ye Q (2006) Electrochim Acta 51:5524
293. Baldauf M, Priedel W (2001) J Appl Electrochem 31:781
294. Colmati F, Paganin VA, Gonzalez EB (2006) J Appl Electrochem 36:17
295. Ito T, Kimura K, Kunimatsu M (2006) Electrochem Commun 8:973
296. Hogarth MP, Hards GA (1996) Platinum Metals Review 40:150
297. Liu R, Smotkin ES (2002) J Electroanal Chem 535:49
298. Chan BC, Lin R, Jambunathan K, Zhang H, Chen G, Mallouk TE, Smotkin ES (2005) J Electrochem Soc 152:A594
299. Chrzanowski W, Kim H, Wieckowski A (1998) Catal Lett 50:69
300. Vericat C, Wakisaka M, Haasch R, Bagus PS, Wieckowski (2004) J Solid-State Electrochem 8:794
301. Iwasita-Vielstich T (1991) Adv Electrochem Electrochem Eng (New Ser) 1:127
302. Iwasita T, Nart FC, Vielstich W (1990) Ber Bunsen-Ges Phys Chem 94:1034
303. Krausa M, Vielstich W (1994) J Electroanal Chem 379:307
304. Dalbeck R, Buschmann HW, Vielstich W (1994) J Electroanal Chem 372:251
305. Gasteiger HA, Ross PN Jr, Cairns EJ (1993) Surf Sci 293:67
306. Gasteiger HA, Markovic N, Ross PN Jr, Cairns EJ (1993) J Phys Chem 97:12020
307. Gasteiger HA, Markovic N, Ross PN Jr, Cairns EJ (1994) J Phys Chem 98:617
308. Gasteiger HA, Markovic N, Ross PN Jr, Cairns EJ (1994) Electrochim Acta 39:1825
309. Gasteiger HA, Markovic N, Ross PN Jr, Cairns EJ (1994) J Electrochem Soc 141:1795, 287
310. Ioroi T, Akita T, Yamazaki S-I, Siroma Z, Fujiwara N, Yasuda K (2006) Electrochim Acta 52:491
311. Ross PN Jr (1998) Electrocatalysys. Lipkowski J, Ross PN (eds), Wiley, New York, p 43
312. Leung L-WH, Weaver M (1988) Langmuir 4:1076
313. Chan HYH, Zou S, Weaver MJ (1999) J Phys Chem B 103:11141
314. Park S, Weaver MJ (2002) J Phys Chem B 106:8667
315. Lin WF, Zei MS, Kim YD, Over H, Ertl G (2000) J Phys Chem B 104:6040
316. Lin WF, Christensen PA, Hamnett A, Zei MS, Ertl G (2000) J Phys Chem B 104:6642
317. Wang WB, Zei MS, Ertl G (2001) Phys Chem Chem Phys 3:3307
318. Zheng M-S, Sun S-G (2001) J Electroanal Chem 500:223
319. Gutierrez C, Caram JA, Beden B (1991) J Electroanal Chem 305:289
320. Lin WF, Iwasita T, Vielstich W (1999) J Phys Chem B 103:3250
321. Zheng M-S, Sun S-G, Chen S-P (2001) J Appl Electrochem 31:749
322. Strbac S, Maroun F, Magnussen OM, Behm RJ (2001) J Electroanal Chem 500:479
323. Herrero E, Franaszczuk K, Wieckowski A (1993) J Electroanal Chem 361:269
324. Frelink T, Visscher W, van Veen JAR (1995) Surf Sci 335:353
325. Frelink T, Visscher W, van Veen JAR (1996) Langmuir 12:3702
326. Friedrich KA, Geyzers K-P, Linke U, Stimming U, Stumper J (1996) J Electroanal Chem 402:123
327. Watanabe M, Genjima Y, Turumi K (1997) J Electrochem Soc 144:423
328. Cramm S, Friedrich KA, Geyzers KP, Stimming U, Vogel R (1997) Fresenius' J Anal Chem 358:189
329. Chrzanowski W, Wieckowski A (1998) Langmuir 14:1967
330. Tremiliosi-Filho G, Kim H, Chrzanowski W, Wieckowski A, Grzybowska B, Kulesza P (1999) J Electroanal Chem 467:143
331. Lin W-F, Zei MS, Eiswirth M, Ertl G, Iwasita T, Vielstich W (1999) J Phys Chem 103:6968
332. Friedrich KA, Geyzers K-P, Marmann A, Stimming U, Vogel R (1998) Z Phys Chem 208:137
333. Vigier F, Gloaguen F, Leger JM, Lamy C (2001) Electrochim Acta 46:4331
334. Samjeske G, Xia XY, Baltruschat H (2002) Langmuir 18:4659
335. Friedrich KA, Geyzers KP, Dickinson AJ, Stimming U (2002) J Electroanal Chem 524:261
336. Davies JC, Hayden BE, Pegg DJ (1998) Electrochim Acta 44:1181
337. Jarvi TD, Madden TH, Stuve EM (1999) Electrochem Solid-State Lett 2:224
338. Davies JC, Hayden BE, Pegg DJ (2000) Surf Sci 467:118
339. Iwasita T, Hoster H, John- Anacker A, Lin WF, Vielstich W (2000) Langmuir 16:522
340. Hoster H, Iwasita T, Baumgartner H, Vielstich W (2001) J Electrochem Soc 148(5):A496
341. Davies JC, Hayden BE, Pegg DJ, Rendall ME (2002) Surface Sci 496:110
342. Lu C, Rice C, Masel RI, Babu PK, Waszczuk P, Kim HS, Oldfield E, Wieckowski A (2002) J Phys Chem B 106:9581
343. Waszczuk P, Lu GQ, Wieckowski A, Lu C, Rice C, Masel RI (2002) Electrochim Acta 47:3637
344. Maillard F, Lu G-Q, Wieckowski A, Stimming U (2005) J Phys Chem B 109:16230
345. Spendelow JS, Wieckowski A (2004) Phys Chem Chem Phys 2:5094
346. Chrzanowski W, Wieckowski A (1997) Langmuir 13:5974
347. Herrero E, Feliu JM, Wieckowski A (1999) Langmuir 15:4944
348. Crown A, Moraes IR, Wieckowski A (2001) J Electroanal Chem 500:333
349. Tong YY, Kim HS, Babu PK, Waszczuk P, Wieckowski A, Oldfield E (2002) J Am Chem Soc 124(3):468
350. Waszczuk P, Solla-Gullon J, Kim H-S, Tong YY, Aldaz A, Wieckowski A (2001) J Catal 203:1
351. Chrzanowski A, Wieckowski A (2000) Interfacial electrochemistry: theory, principles and applications. Wieckowski A (ed), Marcel Dekker, New York, p 937
352. Babu PK, Kim HS, Oldfield E, Wieckowski A (2003) J Phys Chem B 107:7595
353. Park S, Wieckowski A, Weaver MJ (2003) J Am Chem Soc 125:2282
354. Lewera A, Zhou WP, Vericat C, Chung JH, Haasch R, Wieckowski A, Bagus PS (2006) Electrochim Acta 51:3950
355. Lee CE, Tiege PI, Xing Y, Nagendran J, Bergens SH (1997) J Am Chem Soc 119:3543
356. Lee CE, Bergens SH (1998) J Phys Chem B 102:193
357. Cao D, Bergens SH (2002) J Electroanal Chem 533:91
358. Cao D, Bergens SH (2003) Electrochim Acta 48:4021
359. Bett JS, Kunz HR, Aldykiewicz AJ Jr, Fenton JM, Bailey WF, McGrath DV (1998) Electrochim Acta 24:3645
360. Friedrich KA, Geyzers KP, Dickinson AJ, Stimming U (2002) J Electroanal Chem 524-525:261

361. Koper MTM, Lukkien JJ, Jansen APJ, van Santen RA (1999) J Phys Chem B 103:5522
362. Mongeot FB, Scherer M, Gleich B, Kopatzki E, Behm RJ (1998) Surface Sci 411:249
363. Iannielo R, Schmid VM, Stimming U, Stumper J, Wallau A (1994) Electrochim Acta 39:1863
364. Massong H, Wang H, Samjeske G, Baltruschat H (2000) Electrochim Acta 46:701
365. Brankovich SR, McBreen J, Adzic RR (2001) J Electroanal Chem 503:99
366. Brankovic SR, Wang JX, Zhu Y, Sabatini R, McBreen J, Adzic RR (2002) J Electroanal Chem 524-525:231
367. Wang J, Marinkovich NS, Zajonz H, Ocko BM, Adzic RR (2001) J Phys Chem 105:2809
368. Marinkovic NS, Wang JX, Zajonz H, Adzic RR (2001) J Electroanal Chem 500:388
369. El-Aziz AM, Kibler LA (2002) Electrochem Commun 4:866
370. Wang JX, Brankovic SB, Zhu Y, Hanson JC, Adzic RR (2003) J Electrochem Soc 150(8):2003
371. Arico AS, Baglio V, Modica E, di Blasi A, Antonucci V (2004) Electrochem Comm 6:164
372. Knutson TL, Smyrl WH (2004) 206 Meeting ECS Abstracts, Honolulu, Hawaii, p 1506
373. Goodenough JB, Hamnett A (1988) J Electroanal Chem 240:133
374. Goodenough JB, Hamnett A, Kennedy BJ, Weeks SA (1987) Electrochim Acta 32:1233
375. Kennedy BJ, Hamnett A (1990) J Electroanal Chem 283:271
376. Wagner BJ, Kennedy BJ, Wagner FE (1990) J Catal 124:30
377. Hamnett A, Weeks SA, Kennedy BJ, Troughton G, Christensen PA (1990) Ber Bunsenges Phys Chem 94:1014
378. Rolison DR, Hagans PL, Swider KE, Long JW (1999) Langmuir 15:774
379. Long JW, Stroud RM, Swider-Lyons KE, Rolison DR (2000) J Phys Chem B 104:9792
380. Kim H, Rabelo de Moraes I, Tremilosi-Filho G, Haasch R, Wieckowski A (2001) Surf Sci 474:L203
381. Frelink T, Visscher W, Cox AP, van Veen JAR (1996) Ber Bunsenges Phys Chem 100:599
382. Viswanathan R, Liu R, Smotkin ES (2002) Rev Sci Instrum 73:2124
383. Dinh HN, Ren X, Garzon FH, Zelenay P, Gottesfeld S (2000) J Electroanal Chem 491:222
384. Thomas SC, Ren X, Gottesfeld S (1999) J Electrochem Soc 146:4354
385. Cleghorn SJC, Ren X, Springer TE, Wilson MS, Zawodzinski C, Zawodzinski TA, Gottesfeld S (1997) Int J Hydrogen Energy 22:1137
386. Sirk AHC, Hill JM, Kung SKY, Birss VI (2004) J Phys Chem B 108:689
387. Lasch K, Hayn G, Jorissen L, Garche J, Besenhardt O (2002) J Power Sources 105:305
388. Lasch K, Jorissen L, Friedrich KA, Garche J (2003) J Solid-State Electrochem 7:619
389. Yang LX, Allen RG, Scott K, Christenson PA, Roy S (2005) Electrochim Acta 50:1217
390. Lu Q, Yang B, Zhuang L, Lu J (2005) J Phys Chem B 109:1715
391. Chen Z, Qiu X, Lu B, Zhang S, Zhu W, Chen L (2005) Electrochem Commun 7:593
392. Bock C, Collier A, MacDougall B (2005) J Electrochem Soc 152:A2291
393. Bock C, Blakely M-A, MacDougall B (2005) Electrochim Acta 50:2401
394. Park I-S, Choi B, Jung D-S, Sung Y-E (2006) Electrochim Acta 52:1683
395. Watanabe M, Saegusa S, Stonehart P (1989) J Electroanal Chem 271:213
396. Gavrilov AN, Savinova ER, Simonov PA, Zaikovskii VI, Cherepanova SV, Tsirlina GA, Parmon VN (2007) Chem Phys Phys Chem 9:5476
397. Rose A, Crabb EM, Qian Y, Ravikumar MK, Wells PP, Wiltshire RJK, Yao J, Bilsborrow R, Mosselmans F, Russell AE (2007) Electrochim Acta 52:5556
398. Miura H, Gonzalez RD (1982) J Catal 74:216
399. Machado SAS, Tanaka AA, Gonzalez ER (1991) Electrochim Acta 36:1325
400. Schmidt TJ, Noeske M, Gasteiger HA, Behm RJ, Britz P, Brijoux W, Bonnemann H (1997) Langmuir 13:2591
401. Dinh HN, Ren X, Garzon FH, Zelenay P, Gottesfeld S (1994) J Electroanal Chem 491:222
402. Paseka I (2006) J Solid-State Electrochem 11:52
403. Iudice de Souza J, Iwasita T, Nart F, Vielstich W (2000) J Appl Electrochem 30:43
404. Jusys Z, Schmidt T, Dubau L, Lasch K, Jorissen L, Garche J, Behm R (2002) J Power Sources 105:297
405. Green CL, Kucernak A (2002) J Phys Chem 106:1036
406. Nagel T, Bogolowski N, Baltruschat H (2006) J Appl Electrochem 36:1297
407. Bock C, MacDougall B (2003) J Electrochem Soc 150(8):E377
408. Lakchminarayanan V, Srinivasan R, Chu D, Gilman S (1997) Surf Sci 392:44
409. Saffarian HM, Srinivasan R, Chu D, Gilman S (1998) Electrochim Acta 44:1447
410. Piela P, Eickes C, Brosha E, Garzon F, Zelenay P (2004) J Electrochem Soc 151:A2053
411. Ferreira PJ, Lao GL, Shao-Horn Y, Morgan D, Makharia R, Kocha S, Gasteiger HA (2005) J Electrochem Soc 152:A2256
412. Pemberton PYu, Plasse P (2005) J Power Sources 144:11
413. Holstein WL, Rosenfeld HD (2005) J Phys Chem B 109:2176
414. Chen W, Sun G, Guo J, Zhao X, Yan S, Tian J, Tang S, Zhou Z, Xin Q (2006) Electrochim Acta 51:2391
415. Vucovic M, Cukman D (1999) J Electroanal Chem 474:167
416. Sugimoto W, Saida T, Takasu Y (2006) Electrochem Commun 8:411
417. Cheng X, Peng C, You M, Liu L, Zhang Y, Fan Q (2006) Electrochim Acta 51:4620
418. Aoki M, Uchida H, Watanabe M (2006) Electrochem Commun 8 (9):1509
419. Lin SD, Hsiao T-C, Chang J-R, Lin AS (1999) J Phys Chem 103:97
420. Denis MC, Gouerec P, Guay D, Dodelet JP, Lalande G, Schulz R (2000) J Appl Electrochem 30(11):1243
421. Papageorgopoulos DC, Kajzer M, de Bruijn FA (2002) Electrochim Acta 48(2):197
422. Santiago EI, Paganin VA, Do Carmo M, Gonzalez ER, Ticianelli EA (2005) J Electroanal Chem 575:53
423. He Ch, Kunz HR, Fenton JM (1997) J Electrochem Soc 144 (3):970
424. He C, Kunz HR, Fenton JM (2003) J Electrochem Soc 150: A1017
425. Venkataraman R, Kunz HR, Fenton JM (2003) J Electrochem Soc 150(3):A278
426. Leng Y-J, Wang X, Hsing I-M (2002) J Electroanal Chem 528:145
427. Zhang J, Datta R (2005) J Electrochem Soc 152(6):A1180
428. Conway BE, Tilak BV (2002) Electrochim Acta 47:3571
429. Camara GA, Ticianelli EA, Mukerjee S, Lee SJ, McBreen J (2002) J Electrochem Soc 149:A748
430. McGovern MS, Waszczuk P, Wieckowski A (2006) Electrochim Acta 51(7):1194
431. Martinez S, Zinola F, Planes G, Guillen-Villafuerte O, Rodriguez JL, Pastor E (2007) J Solid-State Electrochem 11:1521
432. Wee J-H, Lee K-Y (2006) J Power Sources 157:128

433. Breiter M (1967) Electrochim Acta 12:1213
434. Podlovchenko BI, Frumkin AN, Stenin VF (1968) Elektrokhimija 4:339
435. Petrii OA, Pschenichnikov AG (1980) Problemy Elektrokataliza. Bagotsky VS (ed), Moscow, Nauka, p 41
436. Jarvi TD, Stuve EM (1998) Electrocatalysis. Lipkowsky J, Ross PN (eds), Wiley, NY, p 75.
437. Bock C, Blakely M-A, McDoughal B (2005) Electrochim Acta 50:2401
438. Jiang J, Kucernak A (2003) J Electroanal Chem 543:187
439. Arico AS, Baglio V, Di Blasi A, Modica E, Antonucci PL, Antonucci V (2003) J Electroanal Chem 557:161
440. Tripkovic AV, Strbac S, Popovic KD (2003) Electrochem Commun 5(6):484
441. Choi J-H, Park K-W, Kwon B-K, Sung Y-E (2003) J Electrochem Soc 150(7):A973
442. Kawaguchi T, Sugimoto W, Murakami Y, Takasu Y (2004) Electrochem Commn 6(5):480
443. Wu G, Li L, Xu B-Q (2004) Electrochim Acta 50:1
444. Wang X, Hsing I-M (2003) J Electrochem Soc 556:117
445. Sugimoto W, Aoyama K, Kawaguchi T, Murakami Y, Takasu Y (2005) J Electroanal Chem 576(2):215
446. Belgsir EM, Lamy C (1987) J Electroanal Chem 225:281
447. Korzeniewski C, Childers C (1998) J Phys Chem B 102:489
448. Wang H, Wingender C, Baltruschat H, Lopez M, Reetz MT (2001) J Electroanal Chem 309:163
449. Wang H, Lofler T, Baltruschat H (2001) J Appl Electrochem 31:759
450. Gutierrez AC, Pinheiro ALV, Leiva E, Gonzalez ER, Iwasita T (2003) Electrochem Commun 5(7):539
451. Iwasita T (2002) Electrochim Acta 47:3663
452. Batista EA, Malpass GRP, Motheo AJ, Iwasita T (2003) Electrochem Commun 5(10):843
453. Batista EA, Malpass GRP, Motheo AJ, Iwasita T (2004) J Electroanal Chem 571:273
454. De Lima RB, Massafera MP, Batista EA, Iwasita T (2007) J Electroanal Chem 603:142
455. Islam M, Basnayake R, Korzeniewski C (2007) J Electroanal Chem 599:31
456. Gojkovic SL, Vidakovic TR, Durovic DR (2003) Electrochim Acta 48(24):3607
457. Vidakovic T, Christov M, Sundmacher K (2005) J Electroanal Chem 580(1):105
458. Seiler T, Savinova ER, Friedrich KA, Stimming U (2004) Electrochim Acta 49(22-23):3927
459. Lei H-W, Suh S, Gurau B, Workie B, Lin R, Smotkin ES (2002) Electrochim Acta 47:2913
460. Hogarth MP, Ralph TR (2002) Platinum Met Rev 46:146
461. Kauranen PS, Skou E, Munk J (1996) J Electroanal Chem 404:1
462. Sriramulu S, Jarvi TD, Stuve EM (1998) Electrochim Acta 44:1127
463. Sriramulu S, Jarvi TD, Stuve EM (1999) J Electroanal Chem 467:132
464. Nordlund J, Lindberg G (2002) J Electrochem Soc 149:A1107
465. Nordlund J, Lindberg G (2004) J Electrochem Soc 151:A1357
466. Shivhare MR, Allen RG, Scott K, Morris AJ, Martin EB (2006) J Electroanal Chem 595:145
467. Schultz T, Krewer U, Vidakovic T, Pfafferodt M, Christov M, Sundmacher K (2007) J Appl Electrochem 37:111
468. Wasmus S, Wang J-T, Savinell RF (1995) J Electrochem Soc 142:3825
469. Lin WF, Wang JT, Savinell RF (1997) J Electrochem Soc 144:1917
470. Fan Q, Pu C, Ley KL, Smotkin ES (1996) J Electrochem Soc 143:21
471. Fan Q, Pu C, Smotkin ES (1996) J Electrochem Soc 143:3053
472. Lin AS, Kowalak AD, O'Grady WE (1996) J Power Sources 58:67
473. Schmidt VM, Ianniello R, Pastor E, Gonzalez S (1996) J Phys Chem 100:17901
474. Souza JPI, Rabelo FJB, de Moraes IR, Nart FC (1997) J Electroanal Chem 420:17
475. Hable CT, Wrighton MS (1993) Langmuir 9:3284
476. Wang J, Wasmus S, Savinell RF (1995) J Electrochem Soc 142:4218
477. Arico AS, Creti P, Antonucci PL, Antonucci V (1998) Electrochem Solid-State Lett 1:66
478. Lamy C, Belgsier EM, Leger J-M (2001) J Appl Electrochem 31:799
479. Neto AO, Giz MJ, Perez J, Ticianelli EA, Gonzalez CR (2002) J Electrochem Soc 149:A272
480. Camara GA, De Lima RB, Iwasita T (2004) Electrochem Commun 6:812
481. Camara GA, Iwasita T (2005) J Electroanal Chem 578:315
482. Camara GA, De Lima RB, Iwasita T (2005) J Electroanal Chem 585:128
483. Farias MJS, Camara GA, Tanaka AA, Iwasita T (2007) J Electroanal Chem 600:236
484. Farias MJS, Camara GA, Tanaka AA (2007) J Solid State Electrochem 11:1465
485. Leger J-M, Rousseau S, Coutanceau C, Hahn F, Lamy C (2005) Electrochim Acta 50:5118
486. Tarasevich MR, Karichev ZR, Bogdanovskaya VA, Lubnin EN, Kapustin AV (2005) Electrochem Comm 7:141
487. Wang C-H, Shih H-C, Tsai Y-T, Du H-Y, Chen L-C, Chen K-H (2006) Electrochim Acta 52:1612
488. Li G, Pickup PG (2006) Electrochim Acta 52:1033
489. Taneda K, Yamazaki Y (2006) Electrochim Acta 52:1627
490. Antolini E, Colmat F, Gonzalez ER (2007) Electrochem Commun 9:398
491. Dos Anjos DM, Hahn F, Leger J-M, Kokoh KB, Tremiliosi-Filho G (2007) J Solid-State Electrochem 11:1567
492. Peled E, Livshits V, Duvdevani T (2002) J Power Sources 106:245
493. De Lima RB, Paganin V, Iwasita T, Vielstich W (2003) Electrochim Acta 49:2003
494. Wang H, Jusys Z, Behm RJ (2006) J Electroanal Chem 595:23
495. Wang H, Zhao Z, Jusys Z, Behm RJ (2006) J Power Sources 155:33
496. Matsuoka K, Iriyama Y, Abe T, Matsuoka M, Oguni Z (2005) J Electrochem Soc 152:A729
497. Wang JT, Lin WF, Weber M, Wasmus S, Savinell RF (1998) Electrochim Acta 43:3821
498. Nirmala Grace A, Pandian K (2006) Electrochem Commun 8:1340
499. Savadogo O, Yang X (2001) J Appl Electrochem 31:787
500. Liu Y, Mitsushima S, Ota K-I, Kamiya N (2006) Electrochim Acta 51:6503
501. Hibino T, Hashimoto A, Yano M, Suzuki M, Sano M (2003) Electrochim Acta 48:2531
502. Endo K, Nakamura K, Katayama Y, Miura T (2004) Electrochim Acta 49:2503
503. Furuya N, Yamazaki T, Shibata M (1997) J Electroanalyt Chem 431:39
504. Kawaguchi T, Rachi Y, Sugimoto W, Murakami Y, Takasu Y (2006) J Appl Electrochem 36:1117
505. Maillard F, Peyrelade E, Soldo-Olivier Y, Chatenet M, Chainet E, Faure R (2007) Electrochim Acta 52:1958
506. Neburchilov V, Wang H, Zhang J (2007) Electrochem Commun 9:1788
507. Jeon MK, Won JY, Lee KR, Woo SI (2007) Electrochem Commun 9:2163

508. Anderson AB, Grantscharova E (1995) J Phys Chem 99:9149
509. Anderson AB, Grantscharova E, Seong S (1996) J Electrochem Soc 143:2075
510. Anderson AB (2002) Electrochim Acta 47:3759
511. Anderson AB, Neshev NM, Sidik RA, Shiller P (2002) Electrochim Acta 47:2999
512. Desai S, Neurock M (2003) Electrochim Acta 48:3759
513. Cao D, Lu G-Q, Wieckowski A, Wasileski SA, Neurock M (2005) J Phys Chem B 109:11622
514. Housmans THM, Wonders AH, Koper MTM (2006) J Phys Chem B 110:10021
515. Cuesta A (2006) J Am Chem Soc 128:13332
516. Desai SK, Neurock M (2003) Phys Rev B 68:75420
517. Janik MJ, Taylor CD, Neurock M (2006) Abstracts of 57th Annual Meeting of ISE, Edinbourgh, S8-0-14
518. Koper MTM (2004) Surf Sci 548:1
519. Shubina TE, Koper MTM (2006) Electrochem Commun 8:703
520. Liu P, Norskov JK (2001) Fuel Cells 1:192
521. Liu P, Logadottir A, Norskov JK (2003) Electrochim Acta 48:3731
522. Lischka M, Mosch CH, Gross A (2007) Electrochim Acta 52:2219
523. Harting C, Grimminger J, Spohr E (2007) Electrochim Acta 52:2236